Supporting Information

# Phase Transitions in Zeolitic Imidazolate Framework 7: the Importance of Framework Flexibility and Guest-Induced Instability

Pu Zhao,[*] Giulio I. Lampronti,[*] Gareth O. Lloyd,[†] Michael T. Wharmby,[‡]

Sébastien Facq,[*] Anthony K. Cheetham[‡] and Simon A. T. Redfern[*]

[*]Department of Earth Sciences, [†]Department of Chemistry

and [‡]Department of Materials Science and Metallurgy, University of Cambridge

## 1. Synthesis and characterization of ZIF-7-I

*Synthesis*: All chemicals employed were commercially available (Sigma-Aldrich and Acros Organics), with purity of 98 % or above, and were used as received. ZIF-7-I sample was prepared based on the procedure described by Gücüyener *et al.*, 2010[1]: zinc nitrate hexahydrate ($Zn(NO_3)_2 \cdot 6H_2O$, 0.75 g, 2.52 mmol) and benzimidazole (HPhIm, 0.25 g, 2.05 mmol) were first dissolved in fresh dimethylformamide (DMF, 75 ml). The resultant solution was then poured and sealed into a 100 ml teflon-lined Parr Bomb. The Parr Bomb was heated at 400 K for 48 hours. After naturally cooling to room temperature, white platy crystals were isolated after the mother liquor was removed. The average yield was around 0.34 g, 97.15 % based on HPhIm.

*Characterization*: The ZIF-7-I crystal structure was confirmed by X-ray powder diffraction (XRPD) using Bruker D8 Advance X-ray diffractometer equipped with a Sol-X detector, parallel sollerslits, an incident beam monochromator with $CuK\alpha_1$ radiation ($\lambda$=1.5406 Å) and pulse

height amplifier discrimination. The generator was operated at 40 kV and 40 mA. The sample was prepared for analysis by gently grinding the product obtained in an agate mortar and then depositing on a flat-plate sample holder using ethanol. Diffraction data were collected at room temperature in the range of 6-50° (2θ), in θ:2θ mode and step-scan with Δ2θ=0.02°, for 2 seconds per step. The XRPD pattern of ZIF-7-I was compared with the simulated pattern from the model given by Yaghi *et al.*, 2006.[2] The amount of zinc oxide (ZnO) impurity is negligible, probably less than 1 % wt.

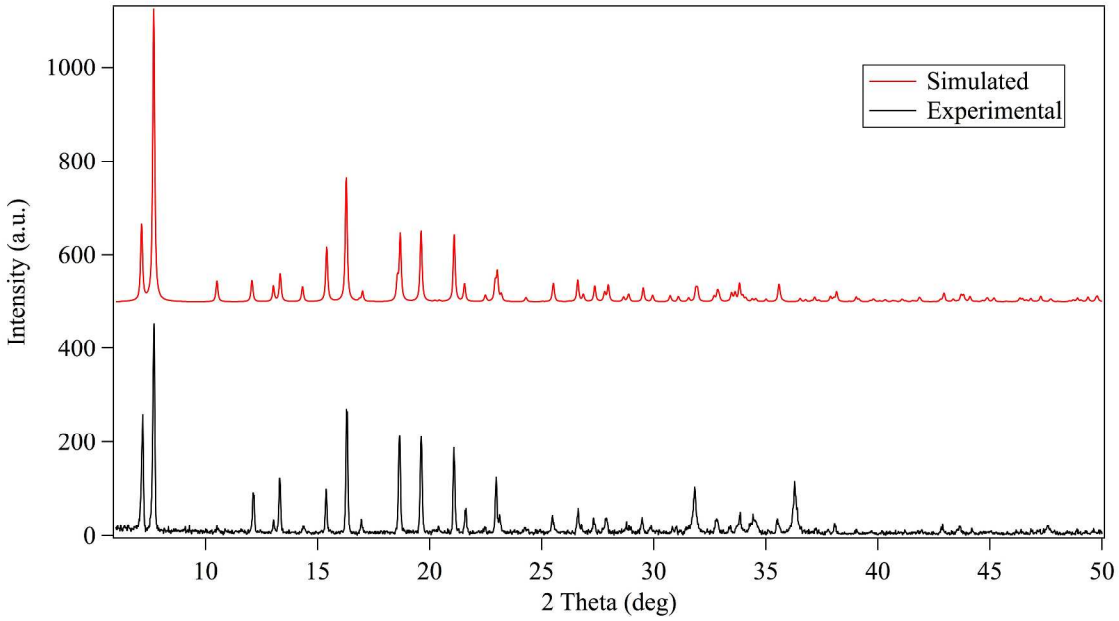


**Figure SI 1.** The simulated and experimental XRPD patterns of ZIF-7-I.

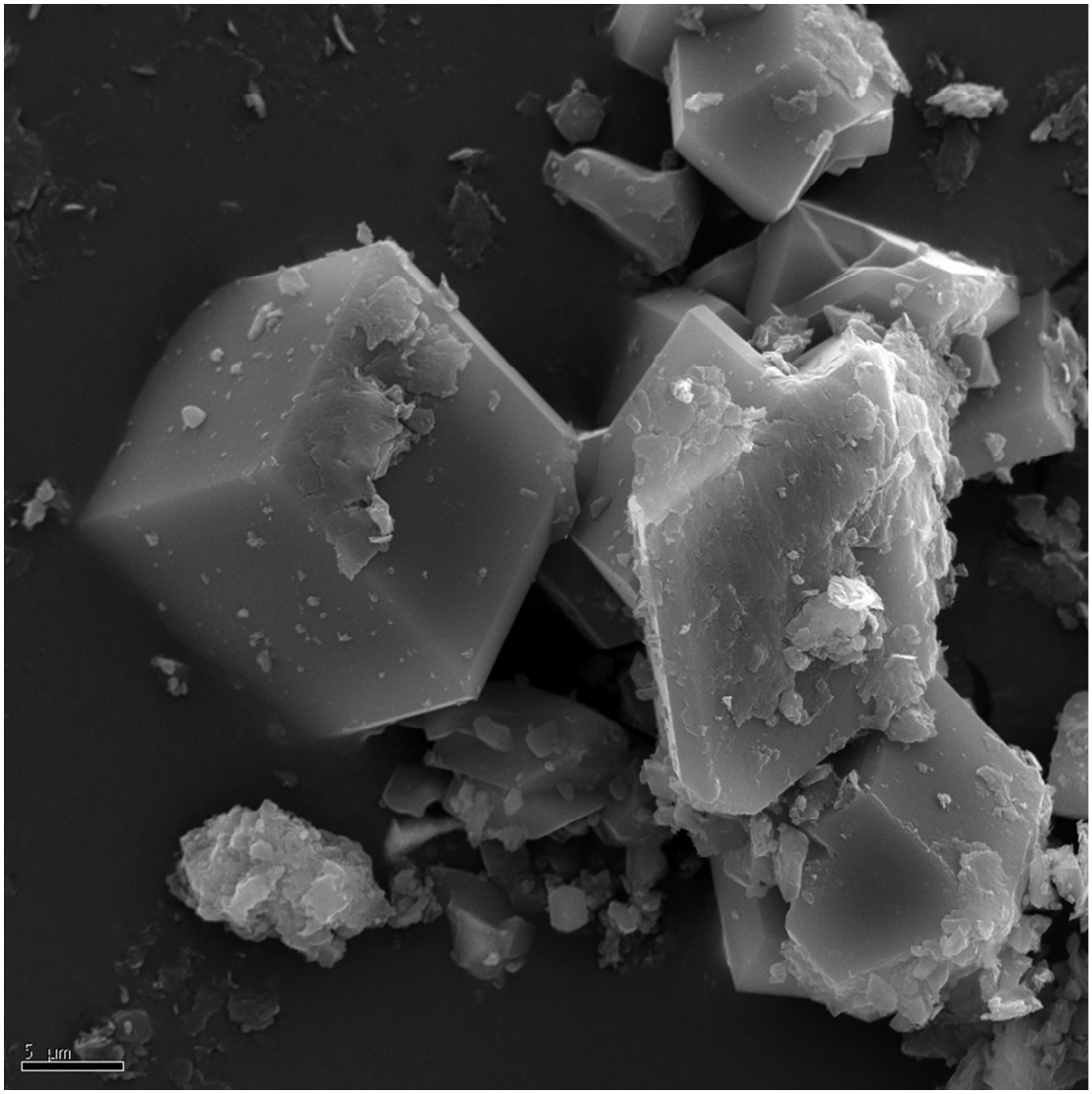


**Figure SI 2.** The scanning electron microscope (SEM) image of as-synthesized ZIF-7-I.

## 2. ZIF-7-I to II phase transition observed by Raman spectroscopy

Raman spectra of an as-synthesized ZIF-7-I sample were collected using a Labram 300 spectrometer (Horiba Jobin-Yvon$^{TM}$) of 300 mm focal length equipped with an 1800 grooves/mm grating and a 1024×256 pixels Peltier cooled CCD detector. The excitation radiation at 632.8 nm was produced by an internal HeNe 20mW laser. Before the experiment, a piece of silicon single crystal was used for calibration. ZIF-7-I sample was placed in a Linkam

TH1500 heating stage under an Olympus™ 50× objective (0.5 N.A.). The temperature of the sample was monitored by a K-type thermocouple placed as close as possible to the sample. In the study, the temperature ranged from 297 to 421 K and was increased by 1 K/min. Raman spectra were collected every 10 K. Typical accumulation time was 60 seconds for each spectrum. Raman spectra were fitted using PeakFit 4.12 in sections; baseline was corrected and the peak features were determined with Voigt function.

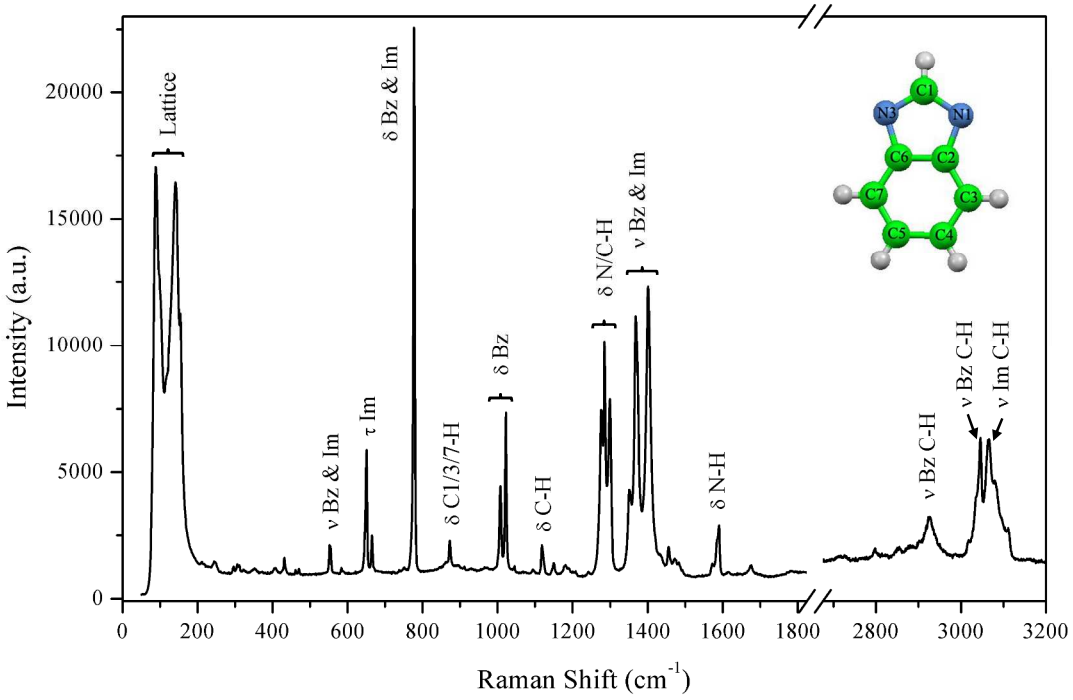


**Figure SI 3.** The Raman spectrum of ZIF-7-I collected at 305 K. ν: stretching; δ: in-plane bending; τ: torsion. Bz: benzene ring; Im: imidazole ring. Inset shows the atom nomenclature used for benzimidazolate, N: blue; C: green; H: silver.

**Table SI 1.** Raman band assignments of ZIF-7-I.

| **Wavenumber ($cm^{-1}$)** | **Band assignment** |
|---|---|
| 87 | Lattice |
| 99 | Lattice |

| | |
|---|---|
| 125 | Lattice |
| 142 | Lattice |
| 551 | ν Bz & Im |
| 554 | νBz & Im |
| 636 | τ Im;<br>mainly Im C-H & N-H wags (asymmetric) |
| 647 | τ Im |
| 650 | τ Im |
| 665 | τ Im |
| 773 | δ Bz & Im<br>angle bending & bond stretching (symmetric) |
| 777 | δ Bz & Im |
| 780 | δ Bz & Im |
| 871 | δ C1-H, C3-H, C7-H |
| 1007 | δ Bz |
| 1021 | δ Bz |
| 1118 | δ C-H |
| 1268 | δ Im X-H, Bz C-H (symmetric) |
| 1276 | δ Im X-H, Bz C-H (symmetric) |
| 1298 | δ C-H |
| 1351 | ν Im C-N |
| 1367 | ν Im C-N |
| 1367 | ν Im C-N |
| 1400 | ν Bz C=C |
| 1573 | δ N-H |
| 1586 | δ N-H |

| | |
|---|---|
| 1590 | δ N-H |
| 2900-3000 | ν Bz C-H |
| 3000-3050 | ν Bz C-H |
| 3050-3150 | ν Im C-H |

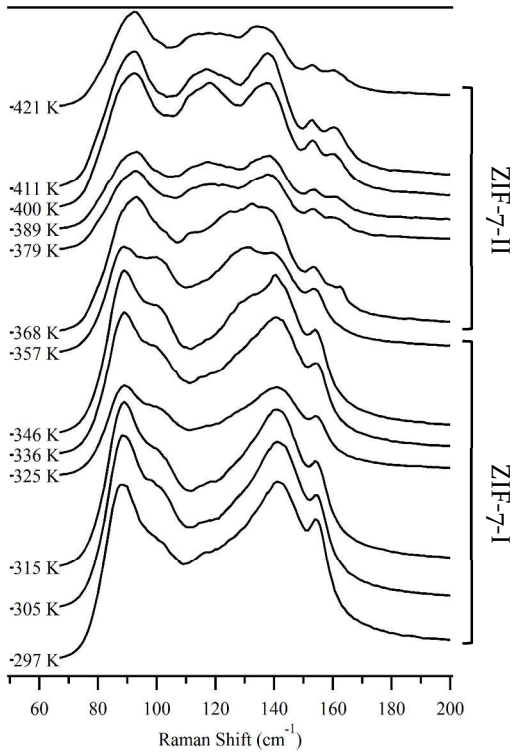


Lattice

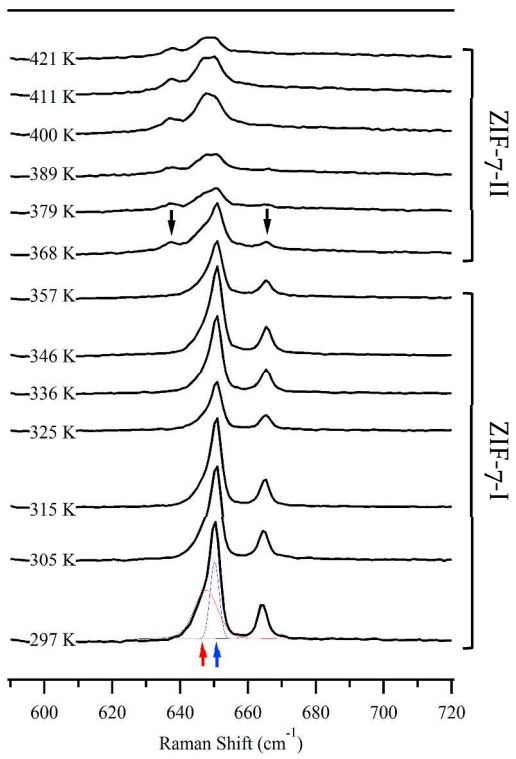
421 K
411 K
400 K
389 K
379 K
368 K
357 K
346 K
336 K
325 K
315 K
305 K
297 K
ZIF-7-II
ZIF-7-I
600 620 640 660 680 700 720
Raman Shift (cm-1)

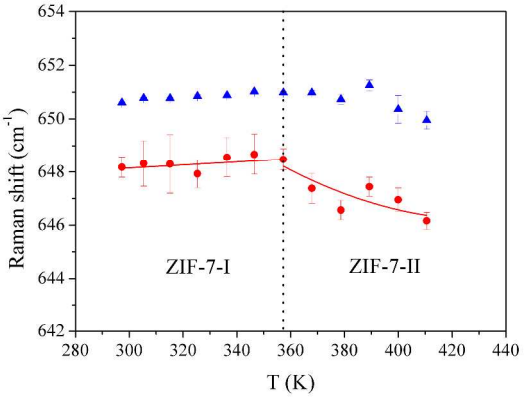
Raman shift (cm-1)
654 652 650 648 646 644 642
ZIF-7-I
ZIF-7-II
280 300 320 340 360 380 400 420 440
T (K)

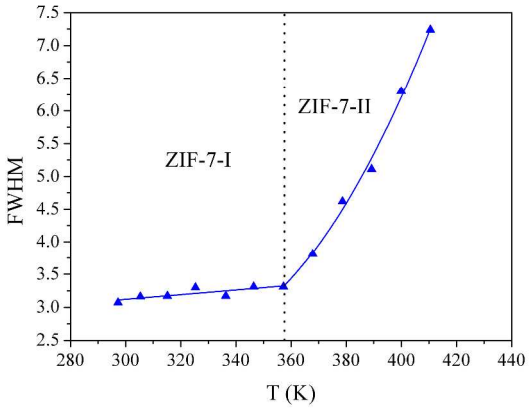
FWHM
7.5 7.0 6.5 6.0 5.5 5.0 4.5 4.0 3.5 3.0 2.5
ZIF-7-I
ZIF-7-II
280 300 320 340 360 380 400 420 440
T (K)

τ Im

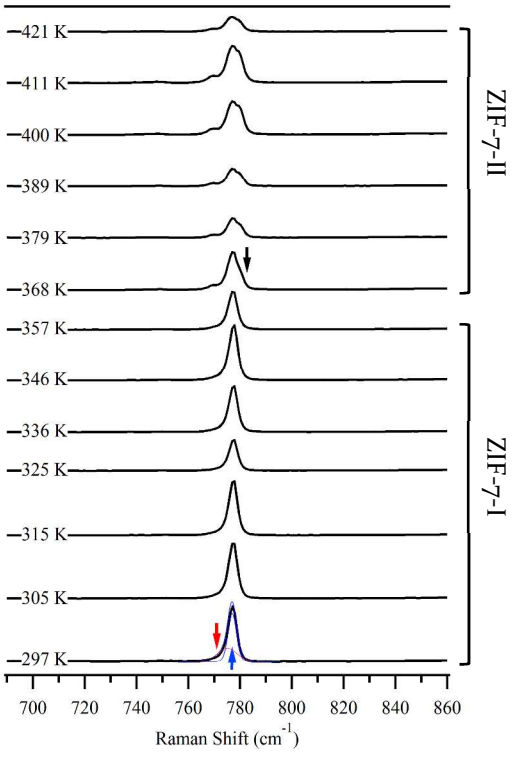
421 K
411 K
400 K
389 K
379 K
368 K
357 K
346 K
336 K
325 K
315 K
305 K
297 K
ZIF-7-II
ZIF-7-I
700 720 740 760 780 800 820 840 860
Raman Shift (cm-1)

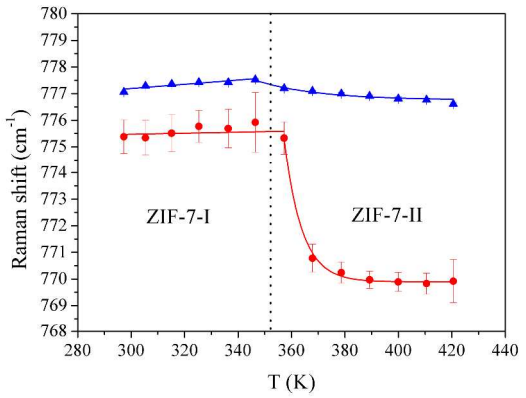
Raman shift (cm-1)
780 779 778 777 776 775 774 773 772 771 770 769 768
ZIF-7-I
ZIF-7-II
280 300 320 340 360 380 400 420 440
T (K)

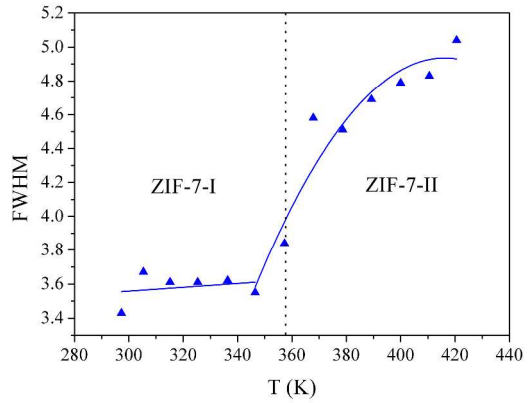
FWHM
5.2 5.0 4.8 4.6 4.4 4.2 4.0 3.8 3.6 3.4
ZIF-7-I
ZIF-7-II
280 300 320 340 360 380 400 420 440
T (K)

δ Bz & Im

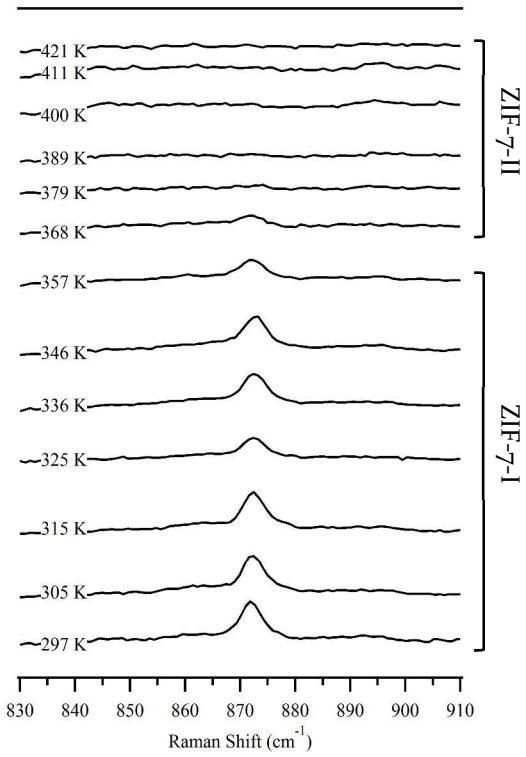


δ C1-H, C3-H, C7-H

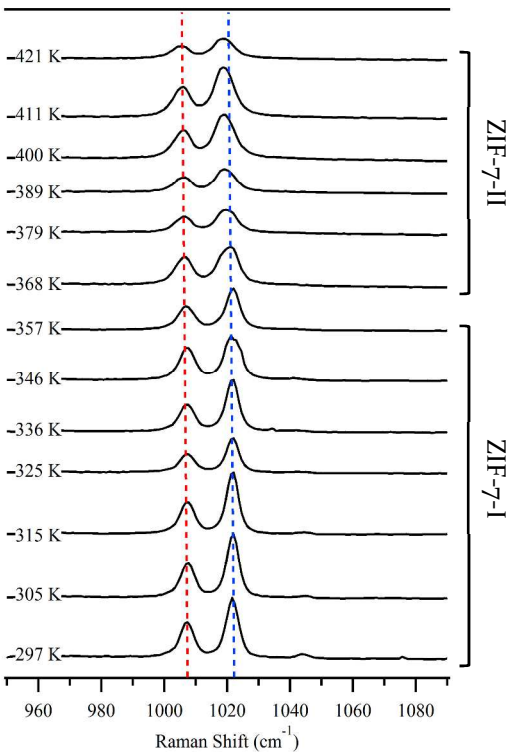


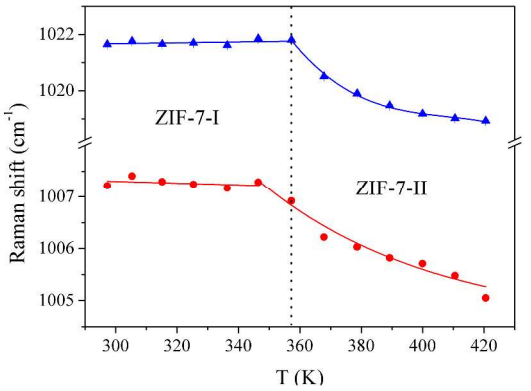


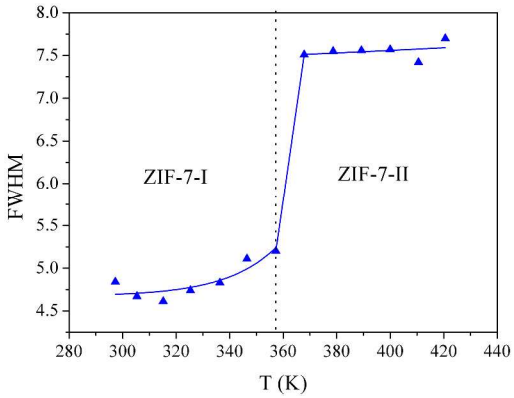


δ Bz

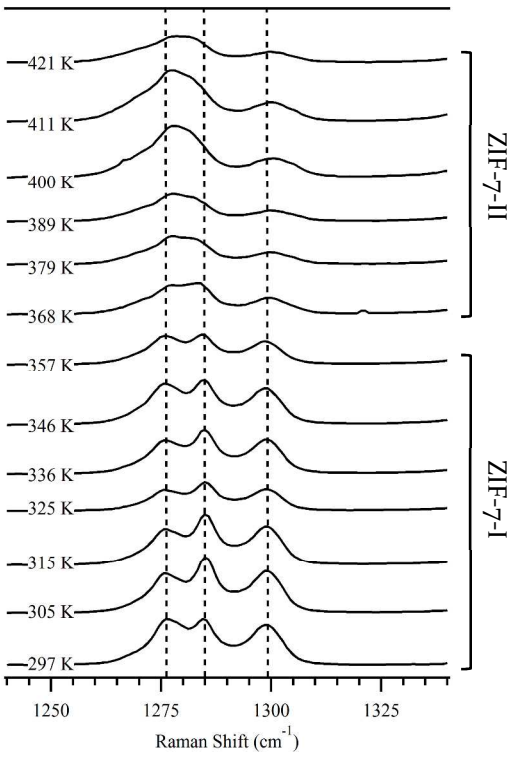


δ Im X-H, Bz C-H (symmetric); δ C-H

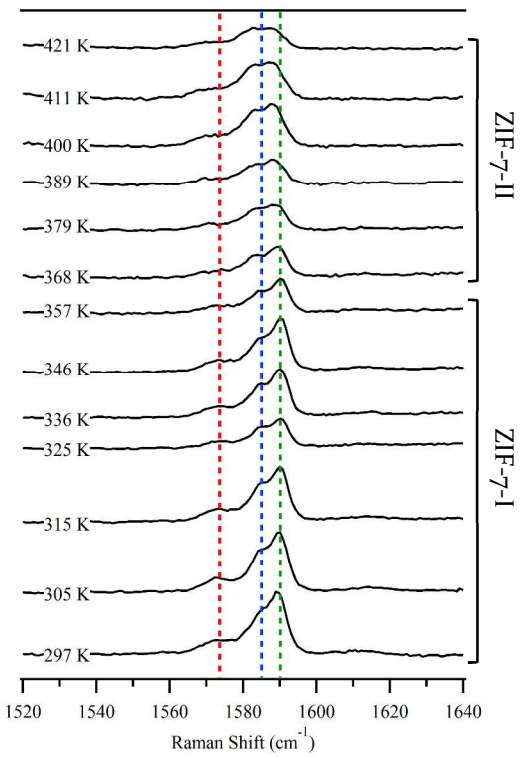


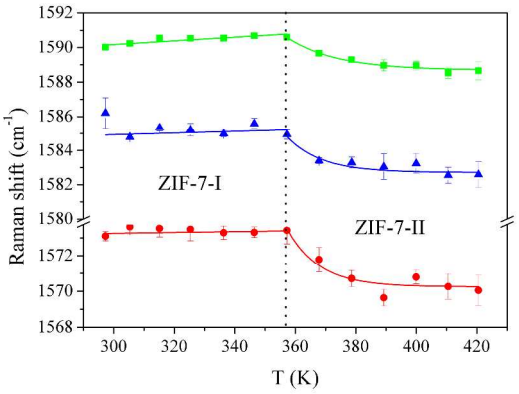


δ N-H

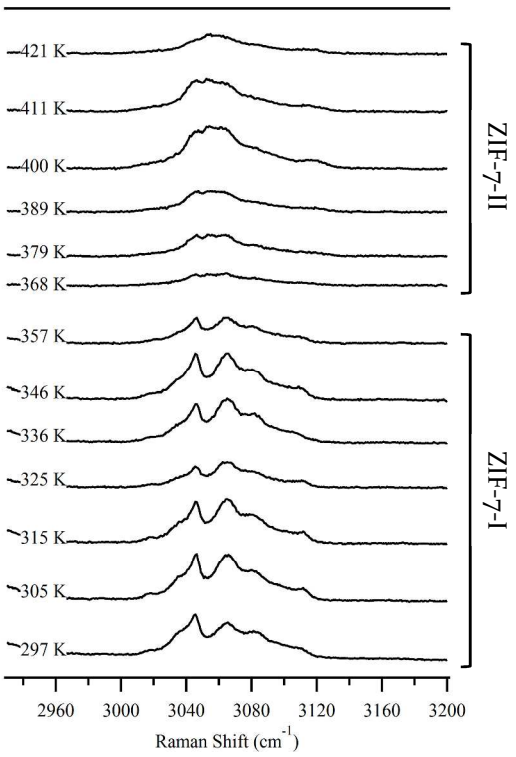


**Figure SI 4.** The Raman spectra evolution. Guide lines to the eyes are added where needed.

## 3. ZIF-7-I and II phase transitions observed by X-ray powder diffraction

High-temperature XRPD study was carried out on an as-synthesized ZIF-7-I sample using Bruker D8 Advance X-ray diffractometer equipped with a VÅNTEC-1 detector and Goeble mirror for parallel beam optics. The generator was operated at 40 kV and 40 mA. The product obtained from solvothermal synthesis was re-homogenized by gently grinding in an agate mortar and then carefully deposited in an alumina sample holder. The sample chamber was evacuated to $10^{-1}$ Pa before analysis using a dynamic vacuum. The diffraction data were collected using CuKα radiation (λ=1.5418 Å) between 6-45° (2θ) in θ:2θ mode and step-scan with Δ2θ=0.02°, for 1 second per step, initially at 300 K and then in temperature steps of 5 K from 300 to 700 K. The delay time for each step was 60 seconds. The diffraction data were also collected at 610, 520, 430 and 340 K during cooling. The same study was performed on another

ZIF-7-I sample that had been exchanged with methanol for 48 hours. As the strongest XRPD peaks of ZIF-7-I and II all appear at 2θ below 25° and the peaks of highly crystallized ZnO impurity dominate the diffraction pattern in 2θ above 25°, only raw data in the 2θ range of 6-25° are shown here. The structure of ZIF-7-II product was re-checked by XRPD after being left in air for two weeks. After ZIF-7-II was immersed in DMF for one week at room temperature, its structure was also double-checked by XRPD.

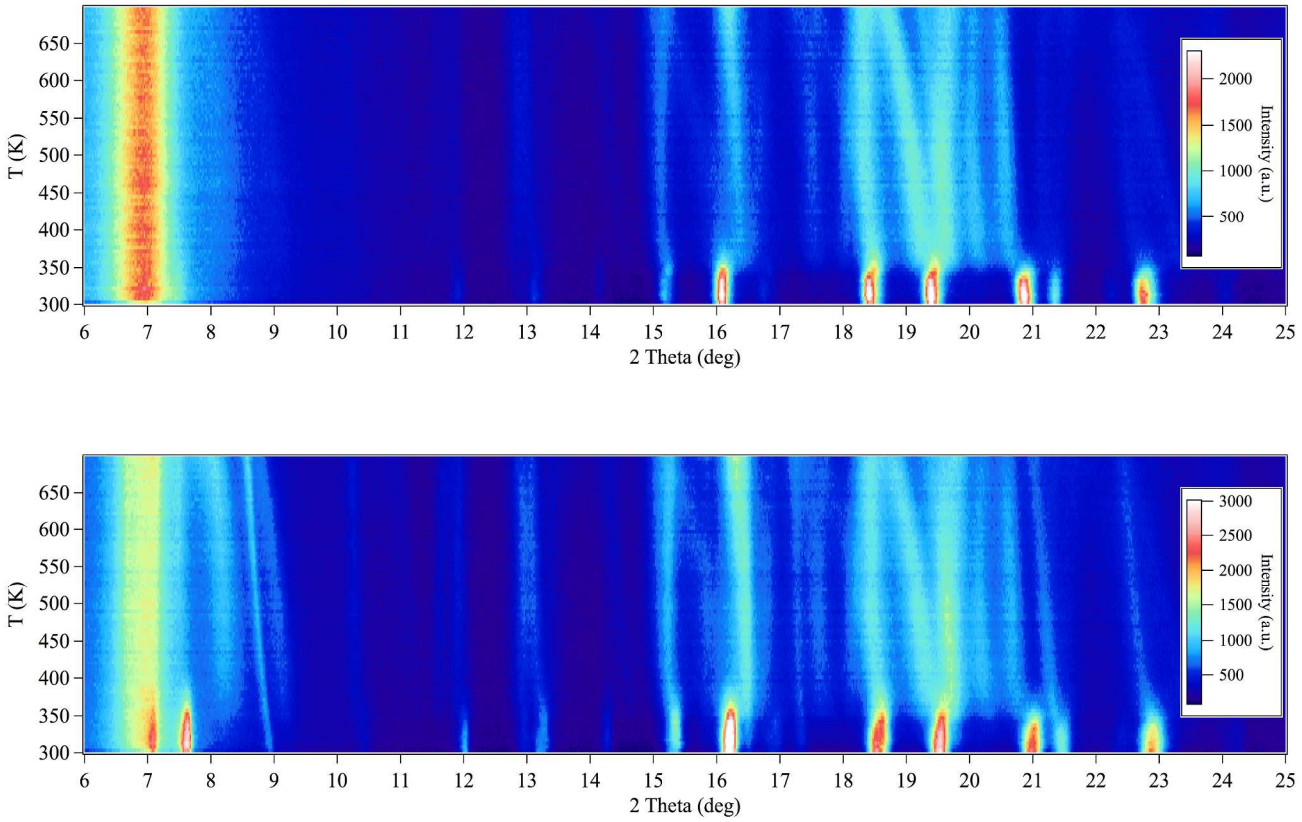


**Figure SI 5.** The high-temperature XRPD patterns of ZIF-7-I. Above: as-synthesized ZIF-7-I; below: methanol-exchanged ZIF-7-I.

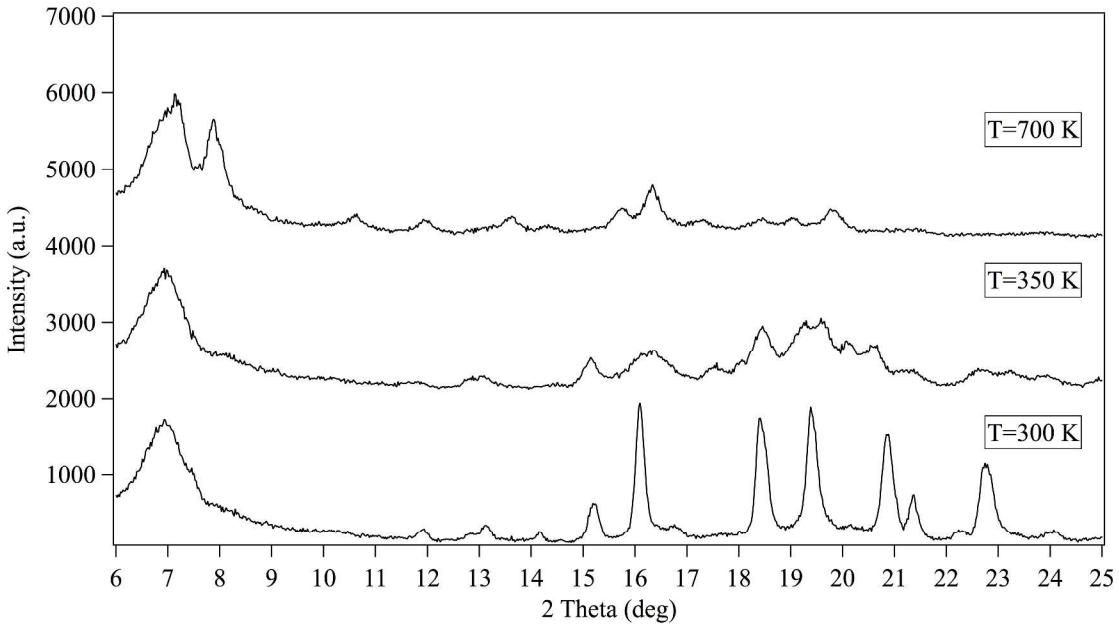


**Figure SI 6.** The high-temperature XRPD patterns of as-synthesized ZIF-7-I at 300, 350 and 700 K.

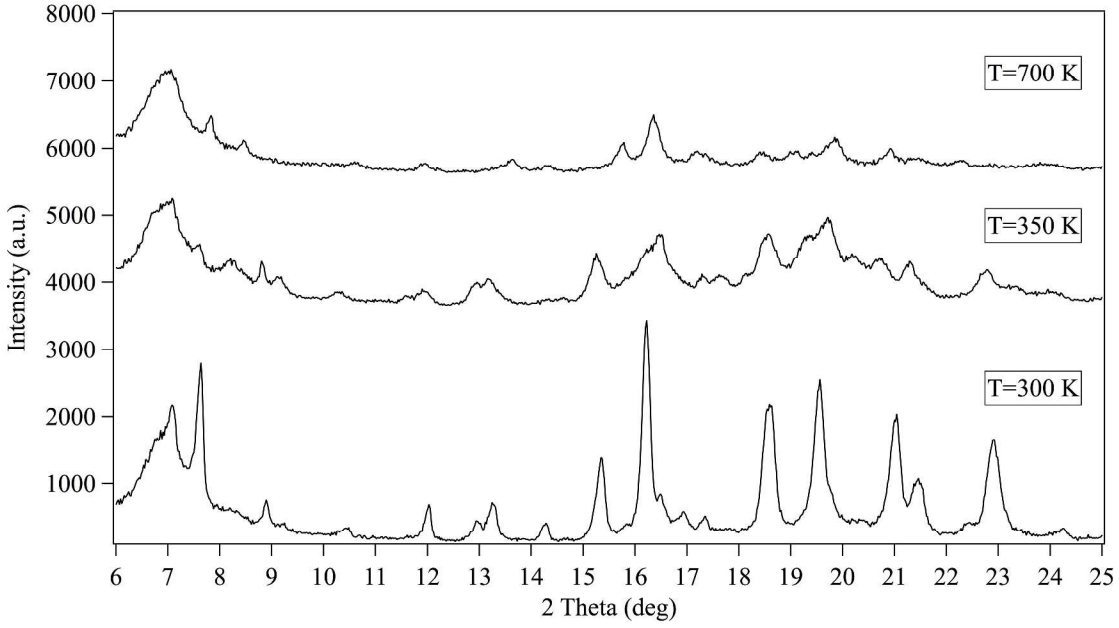


**Figure SI 7.** The high-temperature XRPD patterns of methanol-exchanged ZIF-7-I at 300, 350 and 700 K.

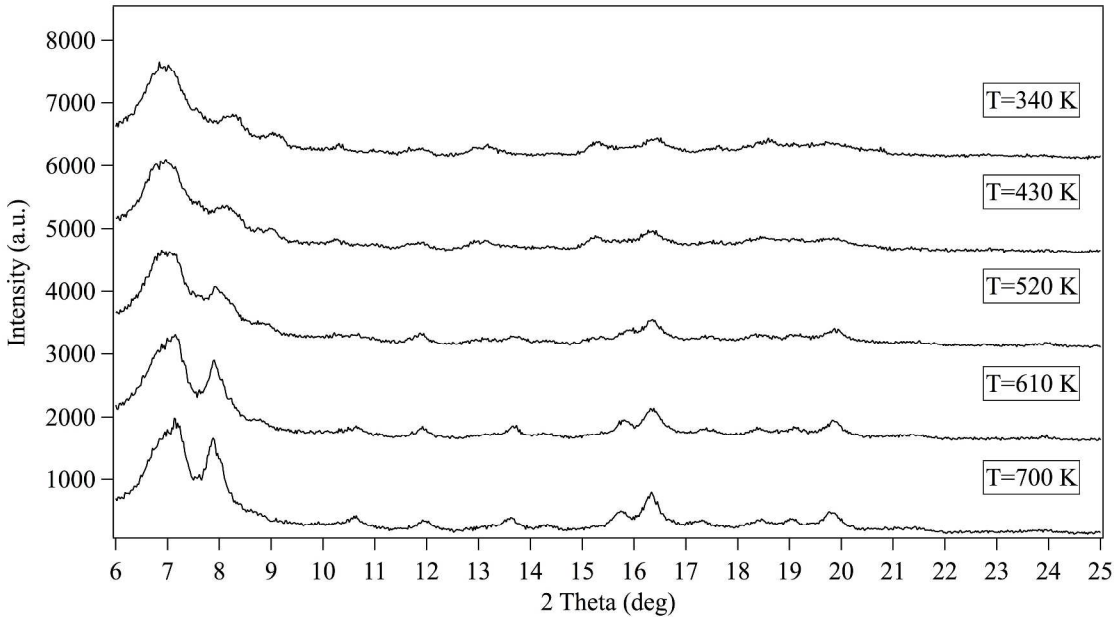


**Figure SI 8.** The high-temperature XRPD patterns of as-synthesized ZIF-7-I at 700, 610, 520, 430 and 340 K during cooling.

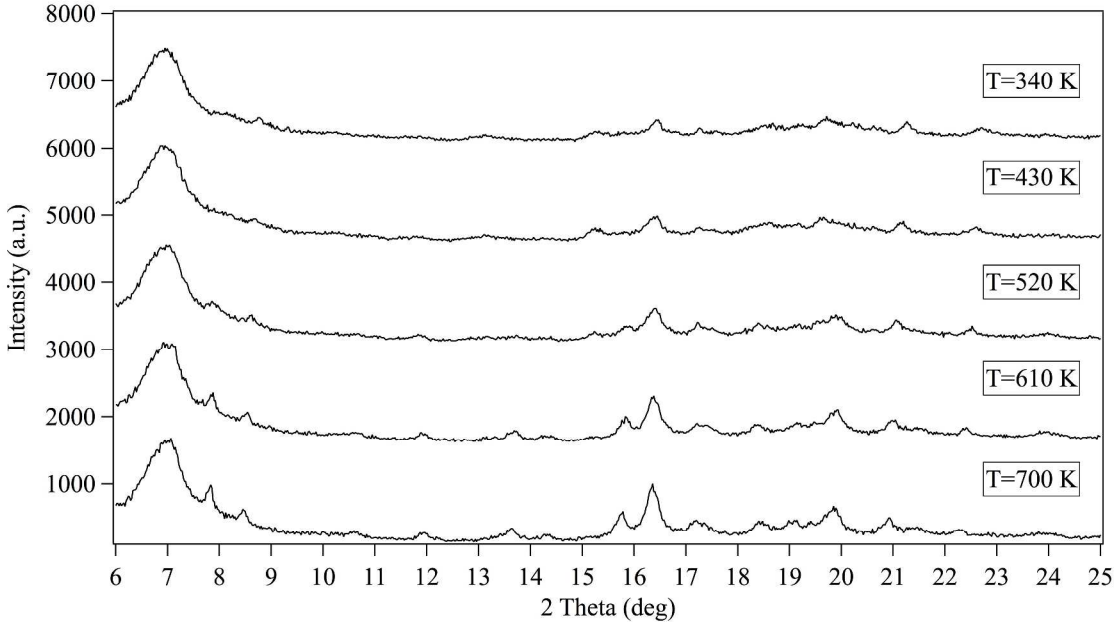


**Figure SI 9.** The high-temperature XRPD patterns of methanol-exchanged ZIF-7-I at 700, 610, 520, 430 and 340 K during cooling.

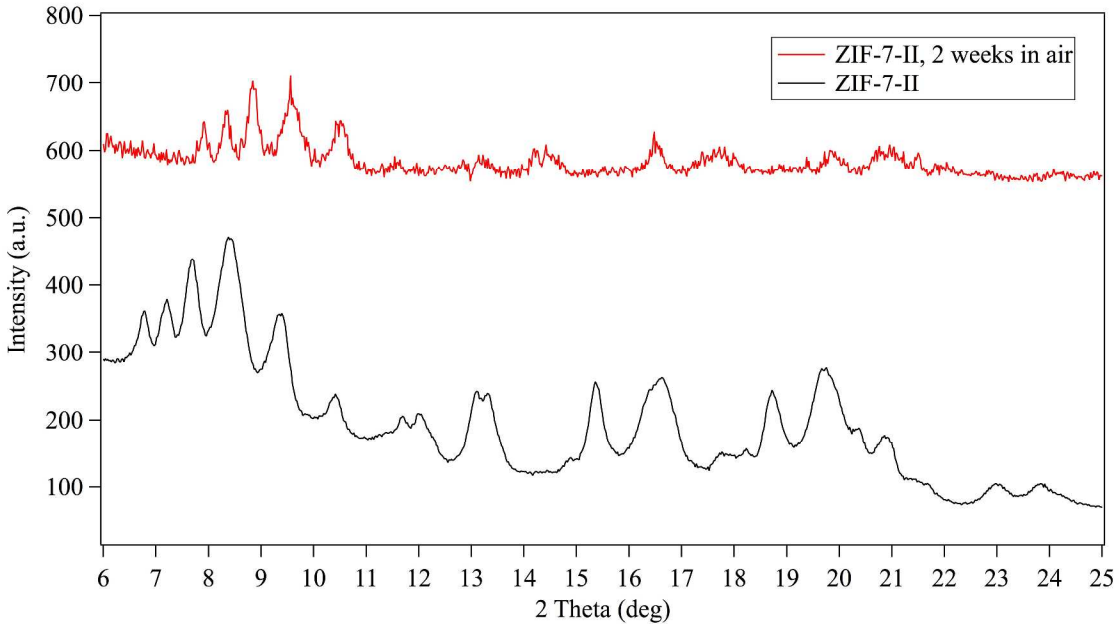


**Figure SI 10.** The XRPD patterns of as-produced ZIF-7-II and ZIF-7-II after being left in air at room temperature for two weeks.

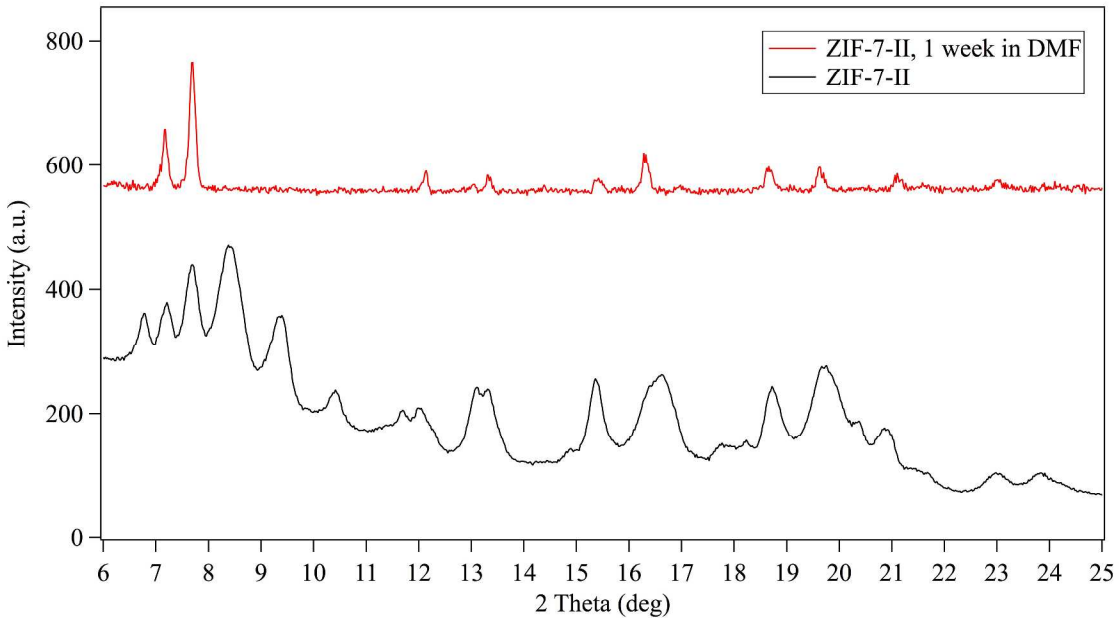


**Figure SI 11.** The XRPD patterns of as-produced ZIF-7-II and ZIF-7-II after being immersed in DMF at room temperature for one week.

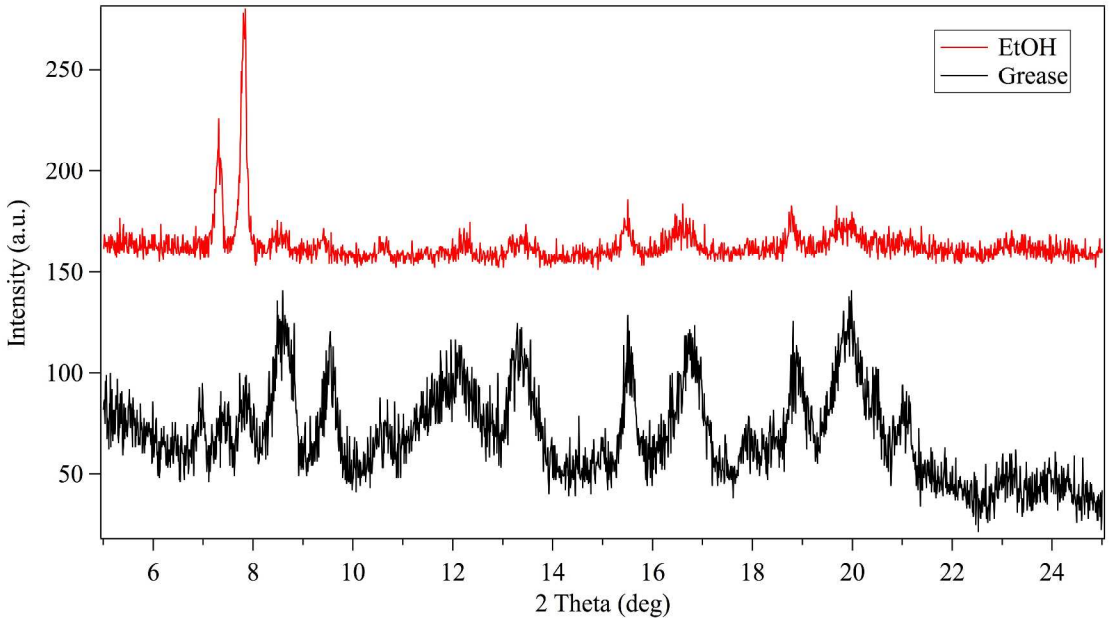


**Figure SI 12.** The XRPD patterns of as-produced ZIF-7-II being deposited on a glass flat-plate using grease and ethanol.

## 4. ZIF-7-I to II phase transition observed by thermogravimetric analysis (TGA) and differential scanning calorimetry (DSC)

TGA analysis was conducted using a Mettler-Toledo TGA/ DSC1/LF/1348 Thermogravimetric Analyzer under a nitrogen atmosphere at a purge rate of 50 ml/min. As-synthesized ZIF-7-I sample was weighed into a 70 µl aluminum pan, before being placed in the analyzer. Sample weight was 21.16 mg. The sample was heated from 298 to 823 K at 5 K/min. The same analysis was conducted on an empty sample pan for background subtraction. STARe was used for data acquisition and analysis.

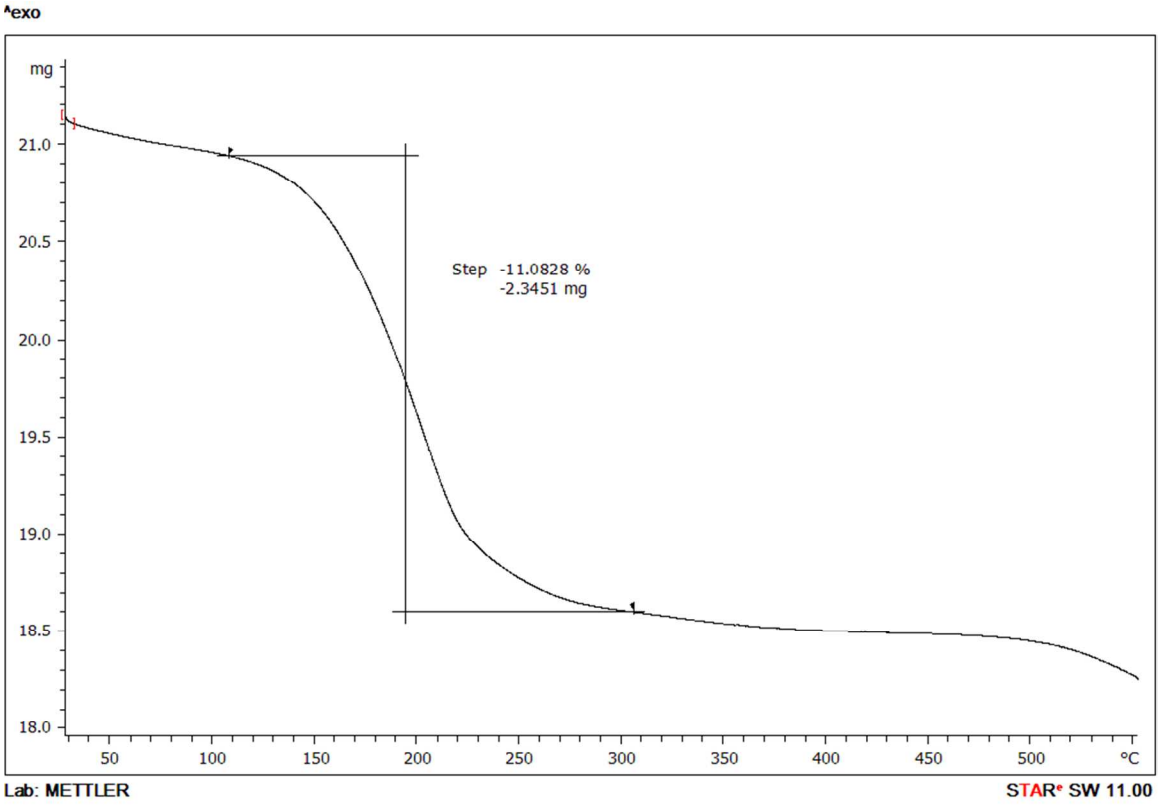


**Figure SI 13.** TGA trace of as-synthesized ZIF-7-I between 298 and 823 K.

DSC analysis was conducted using a Mettler-Toledo DSC822e/700 Differential Scanning Calorimeter under a nitrogen atmosphere at purge rates of 80 and 150 ml/min. As-synthesized ZIF-7-I sample was sealed into a 40 µl aluminum pan with a pin-hole on the cap, before being placed in the calorimeter. Sample weight was 3.57 mg. The sample was heated from 298 to 573 K at 5 K/min. STARe was used for data acquisition and analysis.

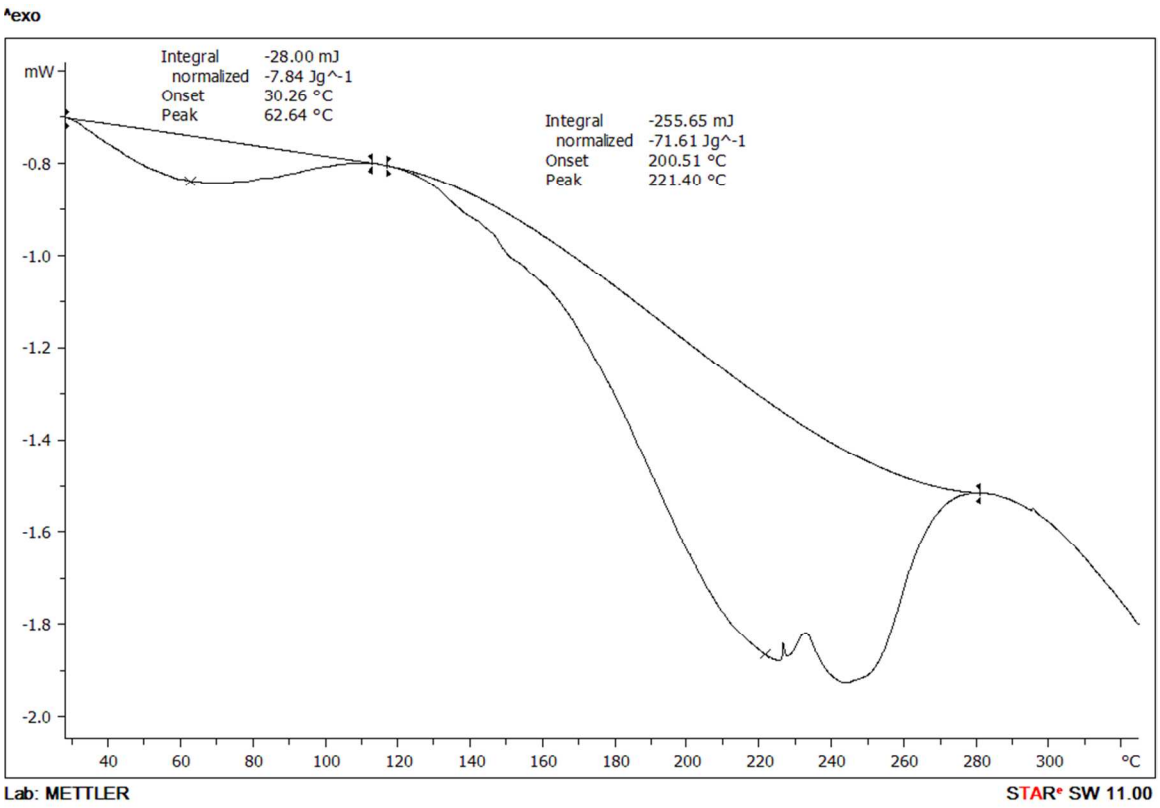


**Figure SI 14.** DSC trace of as-synthesized ZIF-7-I between 298 and 573 K.

DSC analysis was also conducted on ZIF-7-I (MeOH), ZIF-7-II and III samples. Sample weights were 3.61, 3.72 and 3.14 mg, respectively. The samples were heated from 298 to 573 K at 5 K/min.

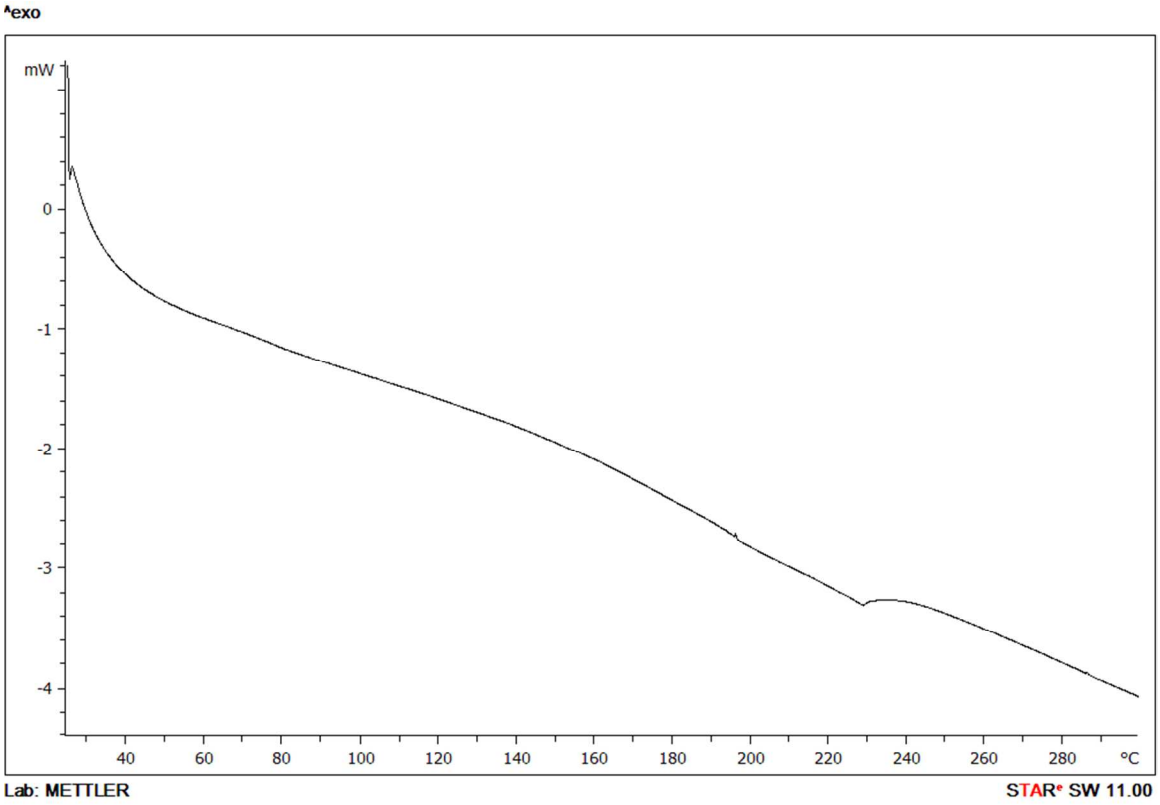


**Figure SI 15.** DSC trace of ZIF-7-I (MeOH) between 298 and 573 K. (The small changes in the curve between 463 and 513 K look more like an instrumental hiccup rather than something physically significant.)

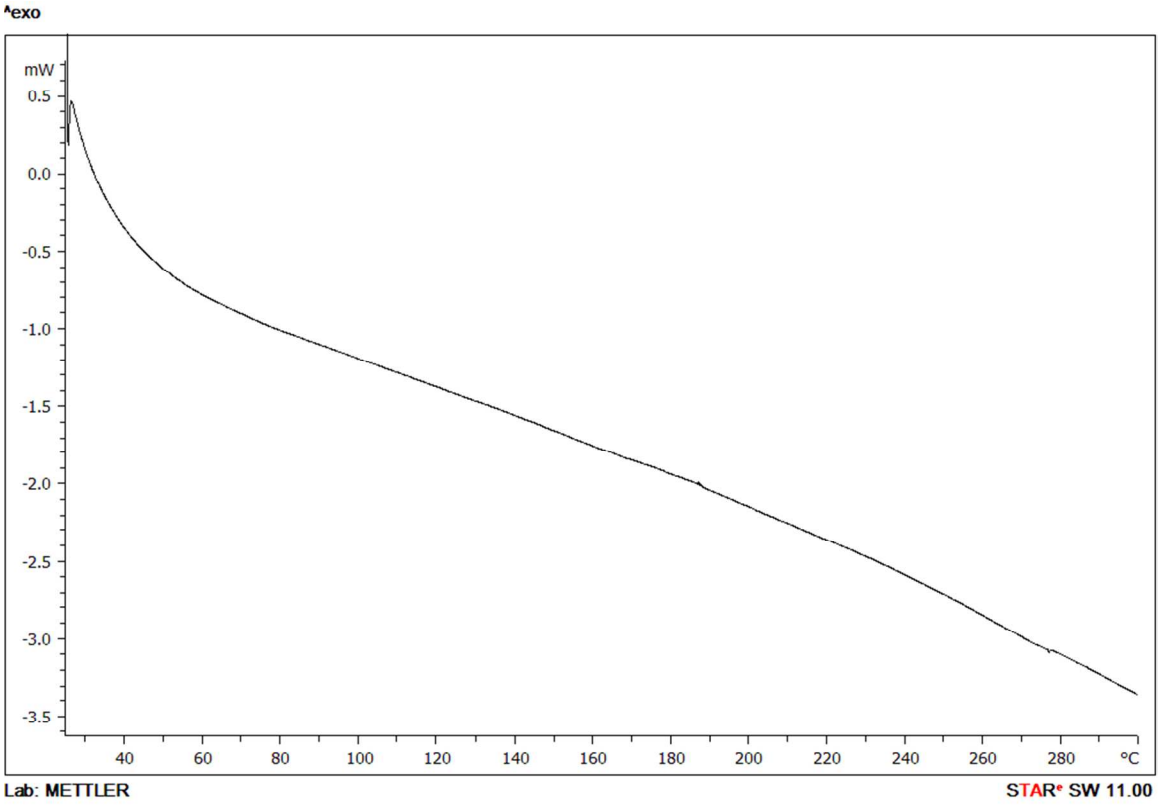


**Figure SI 16.** DSC trace of ZIF-7-II between 298 and 573 K.

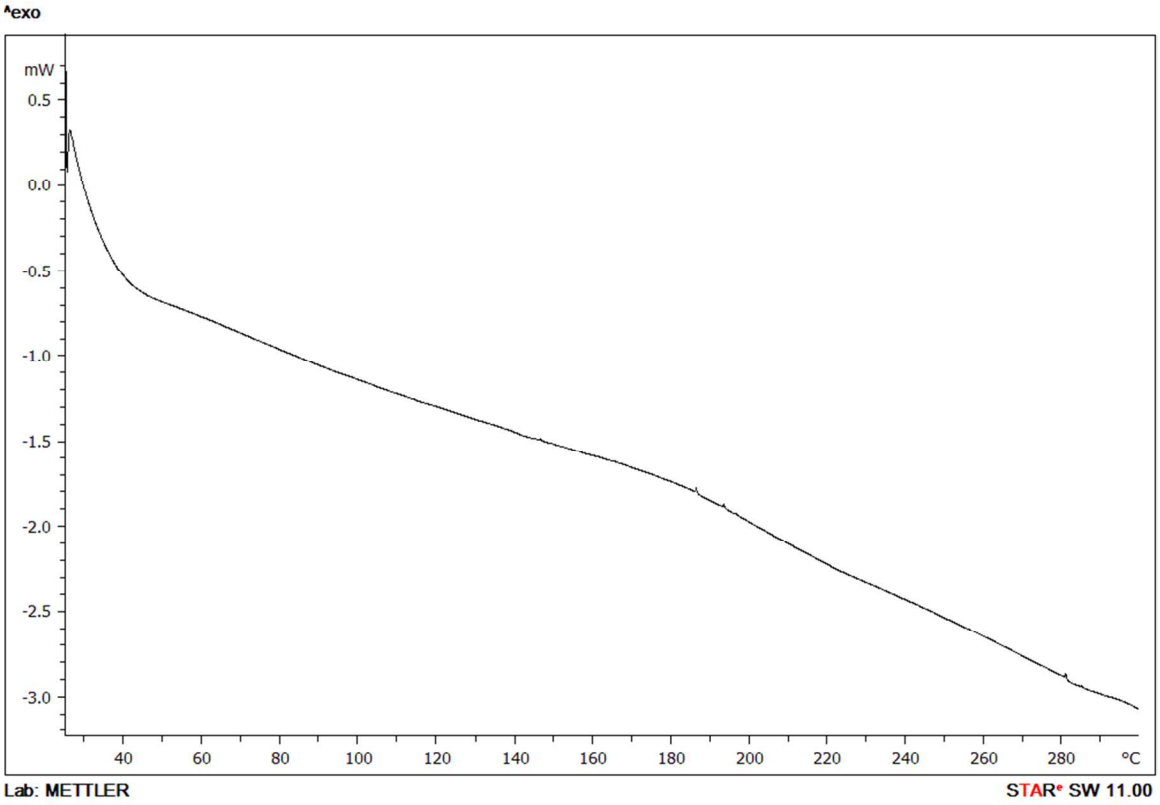


**Figure SI 17.** DSC trace of ZIF-7-III between 298 and 573 K.

## 5. Structure solution of ZIF-7-II using laboratory X-ray powder diffraction

*Production*: ZIF-7-II sample was produced by heating as-synthesized ZIF-7-I at 400 K in air for 48 hours.

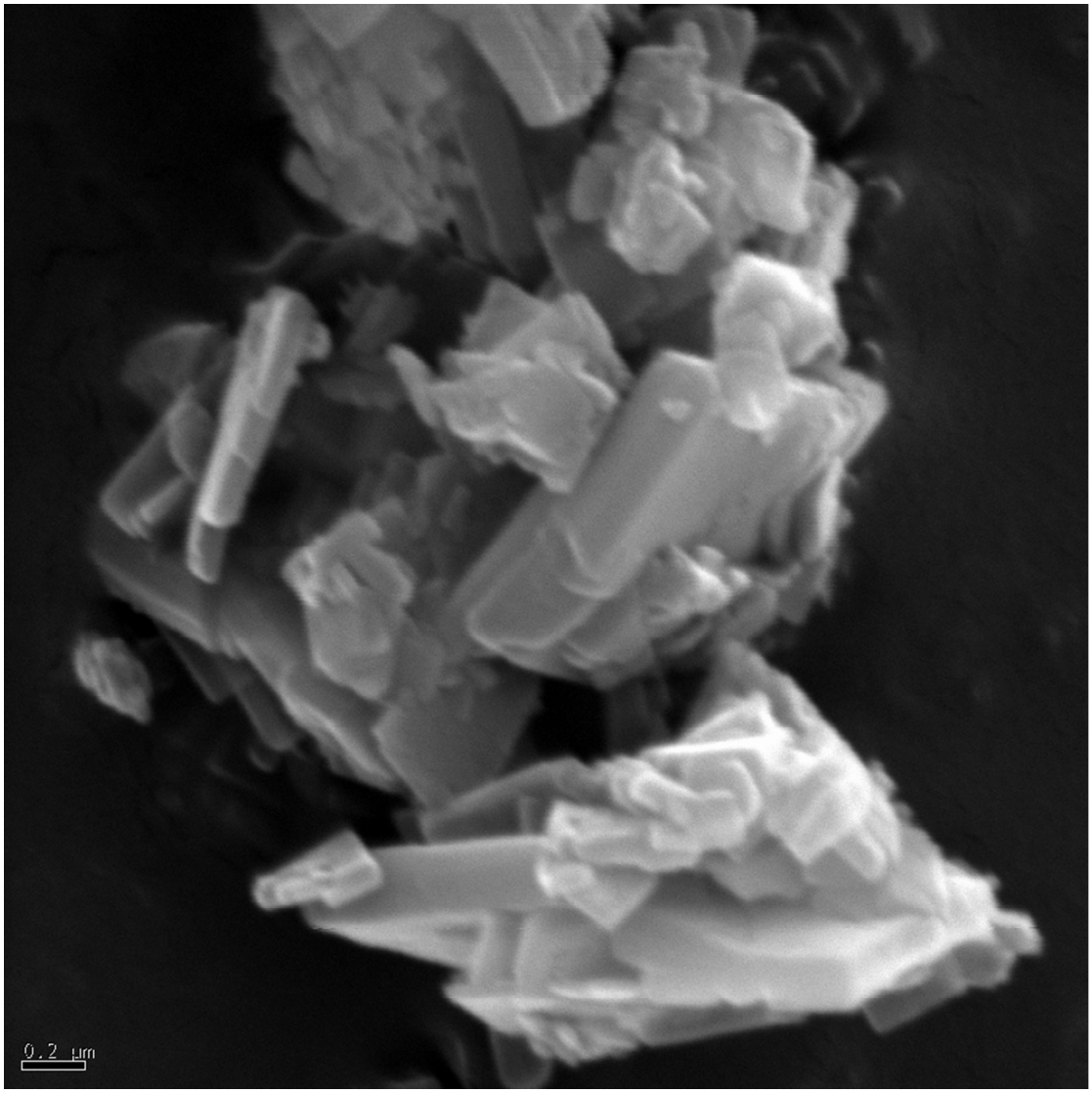


**Figure SI 18.** The SEM image of ZIF-7-II.

*Data collection*: The XRPD data of ZIF-7-II were collected in capillary transmission geometry using a Bruker D8 Advance X-ray diffractometer equipped with a VÅNTEC-1 detector and Goebel mirrors for parallel beam. The generator was operated at 40 kV and 40 mA. The sample was prepared for analysis by gently grinding the product obtained in an agate mortar. Diffraction data were collected at room temperature using CuKα radiation in the range of 5-70° (2θ), and step-scan with Δ2θ=0.02°, for 12 seconds per step.

*Structure solution*: As the peaks of ZnO impurity dominate the diffraction pattern in 2θ above 30° and all refinable XRPD peaks of ZIF-7-II appear at 2θ below 30°, only raw data in the 2θ range of 5-30° are used for structure solution.

Indexing of the powder pattern using Topas-Academic 4.1[3] suggested a metrically monoclinic unit cell, which was refined by the Pawley method[4] to give a cell with $a$ = 23.34910 Å, $b$ = 22.48659 Å, $c$ = 16.23956 Å, γ = 111.52015°, closely related to the hexagonal cell parameters of ZIF-7-I. Structural changes on desolvation tend to follow subgroup/supergroup relationships, i.e. the loss of one or more symmetry operations from the space group due to the distortion of the structure.[5] Thus, since ZIF-7-I crystallizes in the space group *R*-3, the likely space groups for the desolvated structure, ZIF-7-II, are *P*-1, *R*3 or *P*-3. As both *R*3 and *P*-3 fix the angles of the unit cell at α=β= 90°, γ=120°, these two space groups were discarded from further consideration. Starting with the reported structure of ZIF-7-I,[2] solvent molecules were removed and the symmetry was reduced to *P*1. The model was then imported into Material Studio 4.3[6] and the structure was optimized using the Forcite code, allowing all atoms to move under the constraint of fixed connectivity and with the unit cell parameters fixed at the values determined from the Pawley fit. The resulting model was then found to closely match a *P*-1 symmetry, which was used as the starting point for a Rietveld refinement.[7]

The background was described by a 5-term shifted Chebyschev function; two broad Gaussian peaks were necessary to fit the big halo due to the large amorphous fraction. Peak shape was modeled with a pseudo-Voigt function described by CS_L parameter for purely Lorentzian-type crystallite size broadening and Strain_G parameter for microstrain. Spherical harmonics were used for preferred orientation correction. Benzimidazolate ligands were treated as rigid bodies using Cartezian coordinates to reduce the number of variables. Dummy atoms were added to define the origins of rigid bodies. Distance and angle restraints were set between zinc and the coordinating nitrogen atoms with reasonable weight factors. “Anti-bump” restraints were set

between zinc and surrounding carbon and nitrogen atoms with reasonable weight factors. Single isotropic thermal factors were set for the ligands and zinc element respectively.

## 6. Structure refinement of ZIF-7-II using synchrotron X-ray powder diffraction

*Production*: ZIF-7-II sample was prepared by heating the as-synthesized ZIF-7-I at 450 K under dynamic vacuum for 3 hours. The sample was then exposed to air again for approximately one week before being loaded into a 0.7 mm quartz glass capillary. Glass wool was packed on top of the sample and the capillary then fixed onto a custom made gas cell at beamline I11, Diamond Light Source (Harwell, Didcot, Oxfordshire, United Kingdom).[8] The sample was then heated again to 450 K under dynamic vacuum to ensure complete removal of any aerially adsorbed adsorbate molecules.

*Data collection*: The XRPD data of ZIF-7-II were collected in a Debye-Scherrer geometry using X-rays with $\lambda$ = 0.827142 Å at 300 K. The sample was mounted, as described in a custom built gas cell, which prevented spinning of the sample. Instead the sample was rocked through 20° (-10° to 10°) about the $\phi$ axis to improve powder averaging. Data were collected with an array of Mythen II position sensitive detectors over the range 2-90° (2$\theta$), with two data sets offset by 0.25° (2$\theta$) collected (each for 30 seconds). These were subsequently automatically merged to remove gaps in the data where the strips join.

*Rietveld refinement*: All refinable XRPD peaks of ZIF-7-II appear at 2$\theta$ below 30°; only raw data in the 2$\theta$ range of 3-21° are used for structure solution. The background was described by an 8-term shifted Chebyschev function. Peak shape was modeled by Strain_L parameter; an isotropic model was also used to describe the strain broadening.[9] Spherical harmonics were used for preferred orientation correction. Benzimidazolate ligands were treated as rigid bodies to reduce the number of variables. Dummy atoms were added to define the origins of rigid bodies. Thermal factors were not refined. Distance restraints were set between zinc and the

coordinating nitrogen atoms. “Anti-bump” restraints were set between zinc and surrounding carbon and nitrogen atoms with reasonable weight factors. Single isotropic thermal factors were set for the ligands and zinc element respectively.

**Table SI 2.** Crystal data and structure refinement of ZIF-7-II structure.

| | | |
|---|---|---|
| Empirical formula | $C_{14}H_{10}N_4Zn$ | |
| Formula weight | 299.65 | |
| Temperature | 300 K | |
| Wavelength | 0.827142 Å | |
| Crystal system | Triclinic | |
| Space group | *P*-1 | |
| Unit cell dimensions | *a*=23.948(6) Å<br>*b*=21.354(6) Å<br>*c*=16.349(4) Å | α= 90.28(2)°<br>β= 93.28(2)°<br>γ = 108.41(1)° |
| Volume | 7917(3) $Å^3$ | |
| *Z* | 2 | |
| *Z'* | 9 | |
| Density | 1.131 $Mg/m^3$ | |
| 2θ range for data collection | 2-90° | |
| Index range (2θ) | 3-21° | |
| Refinement method | Rietveld refinement method | |
| $R_{wp}$ | 9.96% | |
| $R_{bragg}$ | 4.58% | |
| $Chi^2$ | 22.127 | |

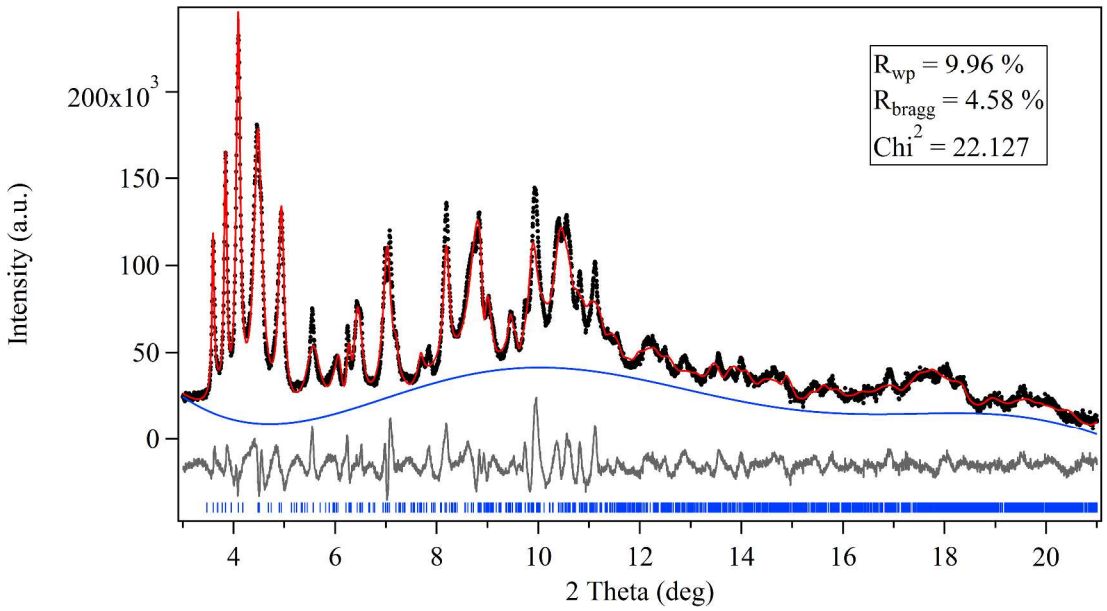


**Figure SI 19.** The observed and calculated XRPD patterns of ZIF-7-II.

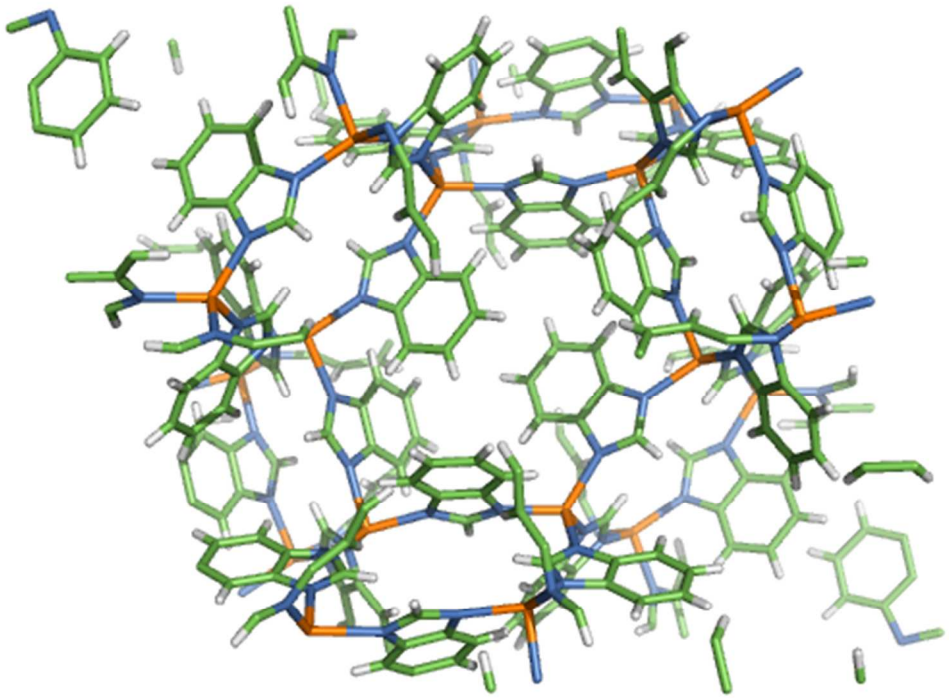

**Figure SI 20.** The structure of ZIF-7-II. Zn: orange; N: blue; C: green; H: silver

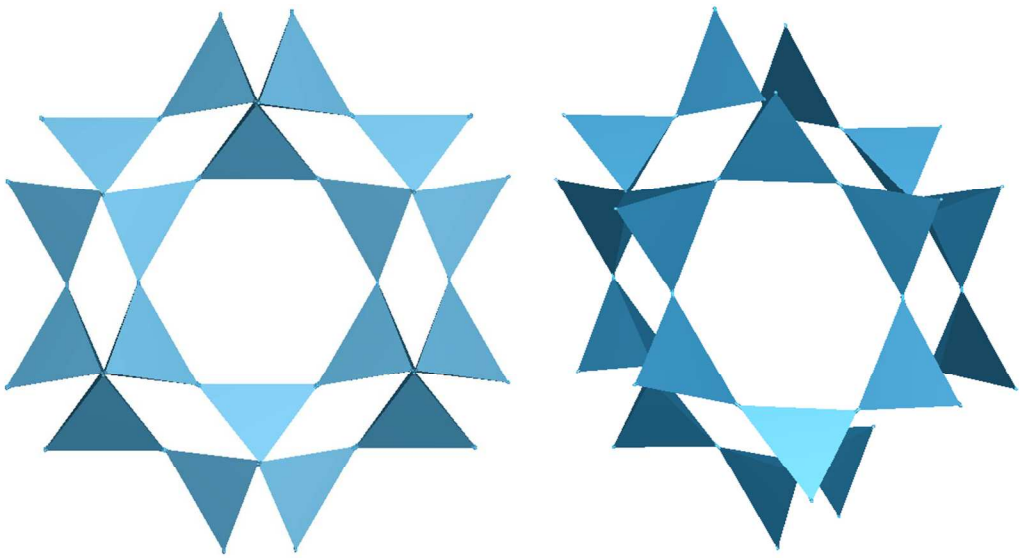

**Figure SI 21.** The structural arrangement of ZIF-7-I (right) and ZIF-7-II (left), displayed as simplified nets of $Zn(PhIm)_4$ vertex-sharing tetrahedra, where each vertex represents a single benzimidazolate molecule. The crystal structures were simplified with Topos 4.0.[10]

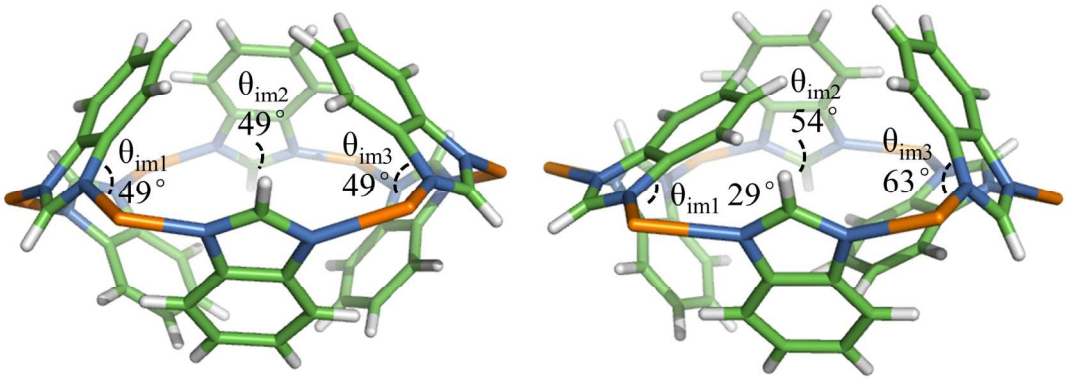


**Figure SI 22.** The structures of the primary guest-hosting cavity in ZIF-7-I and ZIF-7-II with free internal pores. Zn: orange; N: blue; C: green; H: silver.

## 7. ZIF-7-I to III phase transition observed by X-ray powder diffraction

As-synthesized ZIF-7-I was exchanged with methanol for 48 hours and then water for 48 hours; the product was heated at 400 K for 48 hours.

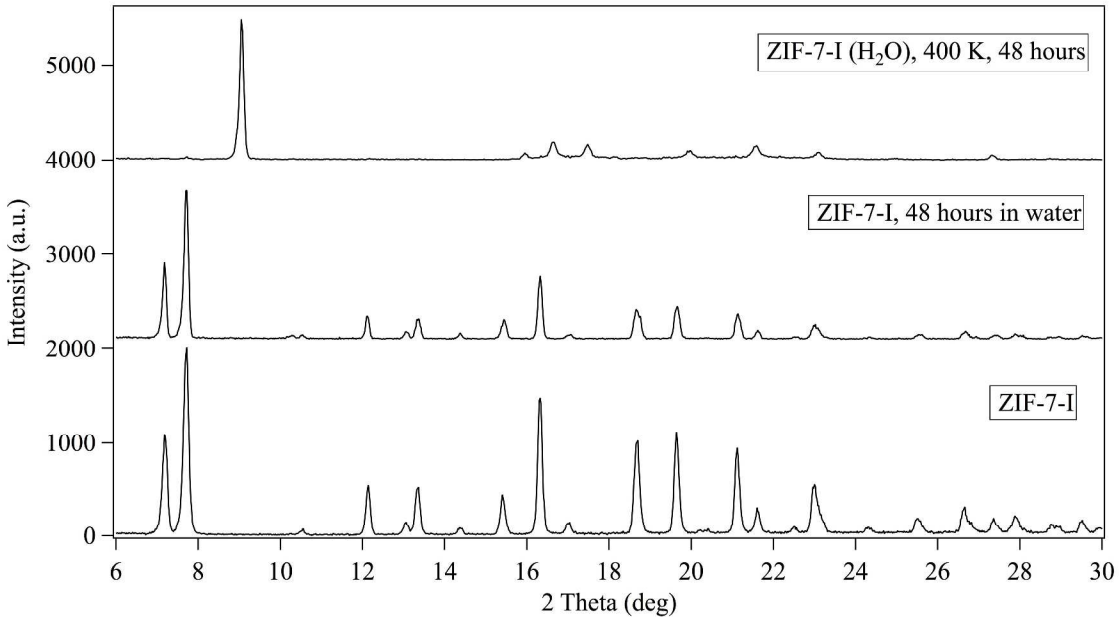


**Figure SI 23.** The XRPD patterns of as-synthesized, water-exchanged ZIF-7-I, and water-exchanged ZIF-7-I after being heated at 400 K for 48 hours.

## 8. ZIF-7-II to III phase transition observed by X-ray powder diffraction

As-produced ZIF-7-II was immersed in water at room temperature for one week.

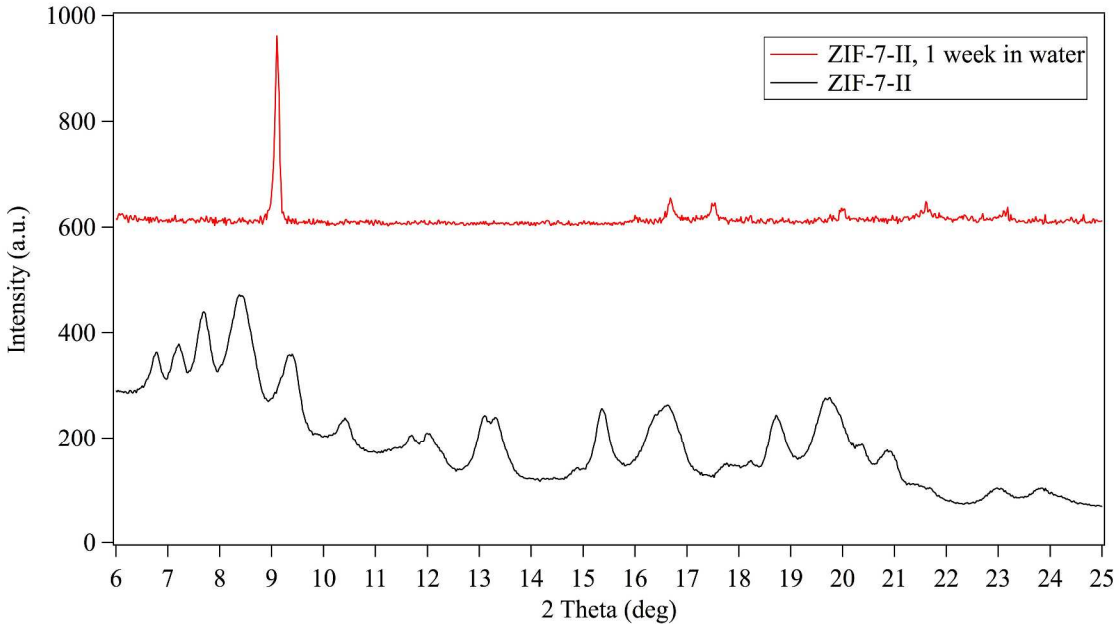


**Figure SI 24.** The XRPD patterns of as-produced ZIF-7-II and ZIF-7-II after being immersed in water at room temperature for one week.

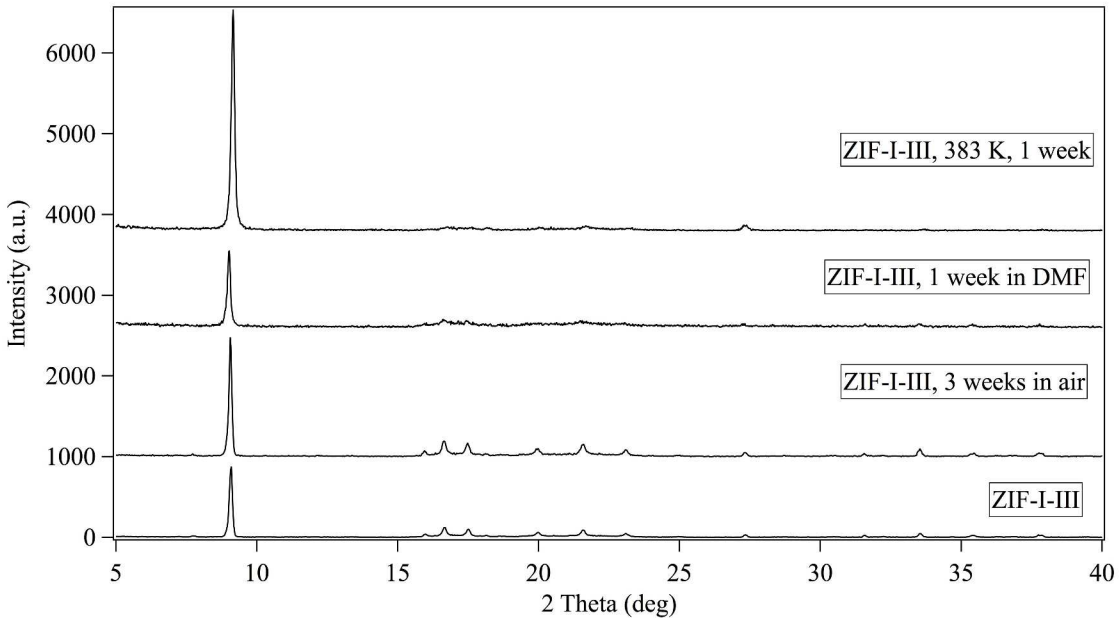


**Figure SI 25.** Stability of ZIF-7-III at room temperature in air and DMF; up to 383 K.

## 9. Synthesis and characterization of ZIF-7-III

*Solvothermal synthesis:* All chemicals employed were commercially available (Sigma-Aldrich and Acros Organics), with purity of 98 % or above, and were used as received. ZIF-7-III sample was synthesized following a similar synthesis procedure with that of ZIF-7-I: $Zn(NO_3)_2 \cdot 6H_2O$ (0.75 g, 2.52 mmol) and HPhIm (0.25 g, 2.05 mmol) were first dissolved in fresh DMF (75 ml). The resultant solution was then poured and sealed into a 100 ml teflon-lined Parr Bomb. The Parr Bomb was heated at 373 K for 48 hours. After naturally cooling to room temperature, white powdery crystals were isolated after the mother liquor was removed. The average yield was around 0.34 g, 97.15 % based on HPhIm.

This synthesis procedure is very unstable and hardly repeatable, following which ZIF-7-I can be occasionally obtained and a compound with chemical formula of $\{[Zn_2(PhIm)_3(OH)(H_2O)] \cdot (DMF)(H_2O)_3\}\infty$ can also be produced. This compound was discovered by Xu *et al.* in 2005[11] and has a 2D layer structure similar with ZIF-7-III, formed by triply linked corner-shared networks of zinc(II) benzimidazolate polymers inserted with hydroxyl and water molecules.

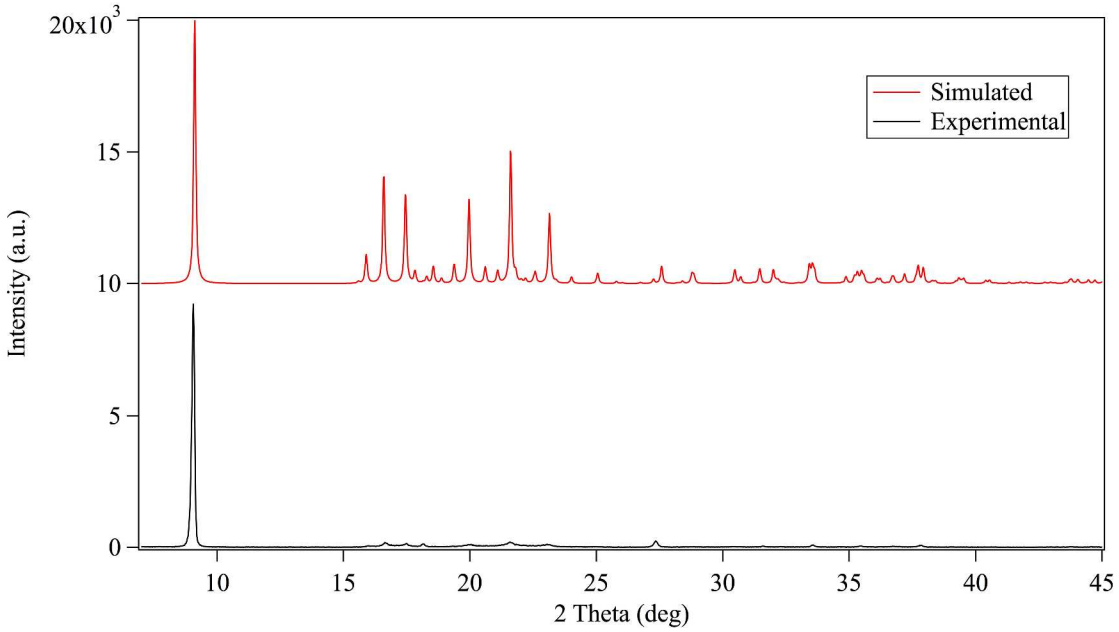


**Figure SI 26.** The simulated and experimental XRPD patterns of ZIF-7-III.

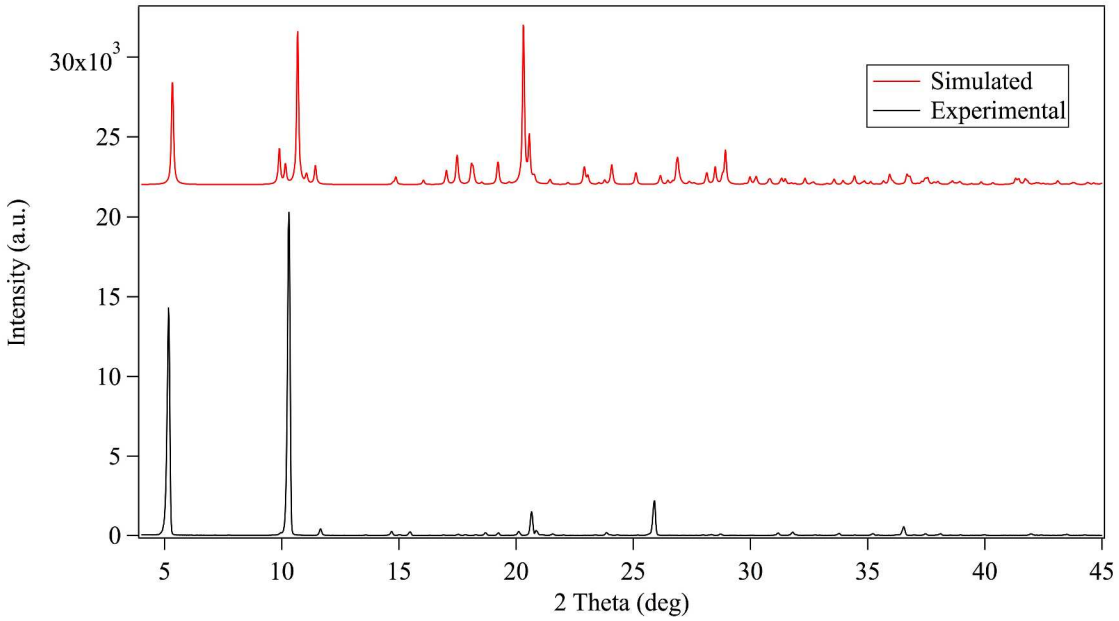


**Figure SI 27.** The simulated and experimental XRPD patterns of $\{[Zn_2(PhIm)_3(OH)(H_2O)]\bullet(DMF)(H_2O)_3\}\infty$.

*Mechanical synthesis:* All chemicals employed were commercially available (Sigma-Aldrich and Acros Organics), with purity of 98 % or above. $Zn(NO_3)_2\bullet 6H_2O$ (88.50 mg, 0.30 mmol), HPhIm (71.45 mg, 0.60 mmol) and sodium bicarbonate ($NaHCO_3$, 47.38 mg, 0.56 mmol) were mixed in a 14.5 mL stainless steel jar along with two 7 mm diameter stainless steel balls. The reagents were then ground for 60 minutes in a Retsch MM400 grinder mill operating at 30 Hz. Product was washed with water to get rid of remaining $NaHCO_3$ and $NaNO_3$. White powdery product was obtained for characterization. The XRPD pattern of ZIF-7-III is compared with simulated pattern from the model given by Yang *et al*., 2008.[12]

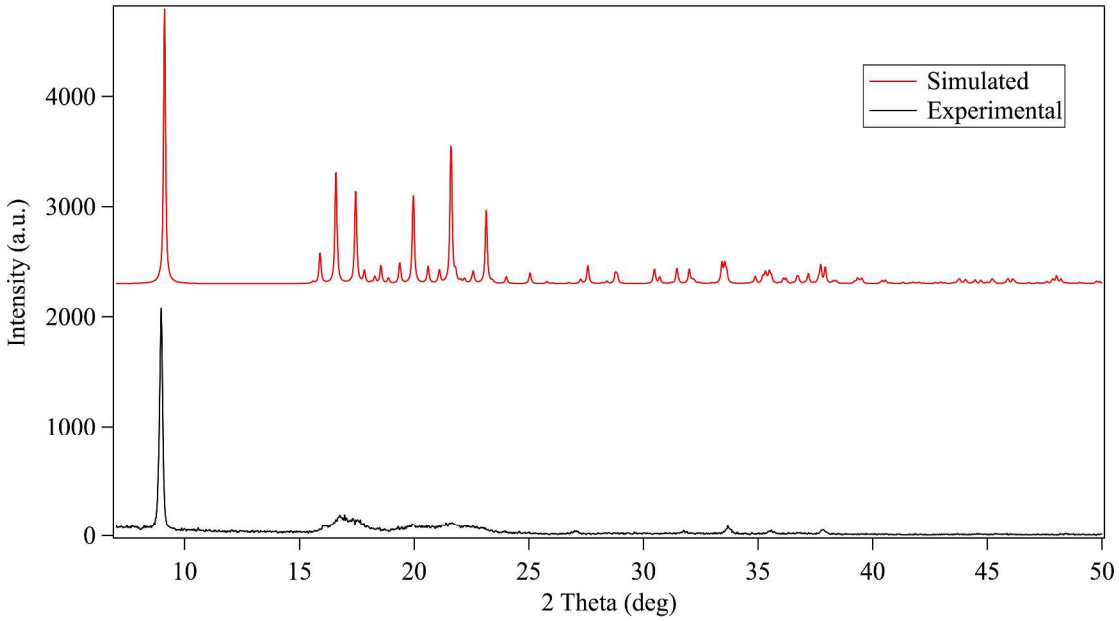


**Figure SI 28.** The simulated and experimental X-ray diffraction patterns of ZIF-7-III obtained from ball milling.

ZIF-7-III can also be easily produced by liquid-assisted manually grinding. $Zn(NO_3)_2 \cdot 6H_2O$ (84.00 mg, 0.28 mmol), HPhIm (69.00 mg, 0.58 mmol) and $NaHCO_3$ (48.40 mg, 0.58 mmol) were mixed in an agate mortar. The reagents were then manually ground under ethanol for 10 minutes. After 2 days drying in air, the product was washed with water to get rid of remaining $NaHCO_3$ and $NaNO_3$. White powdery product was obtained for characterization.

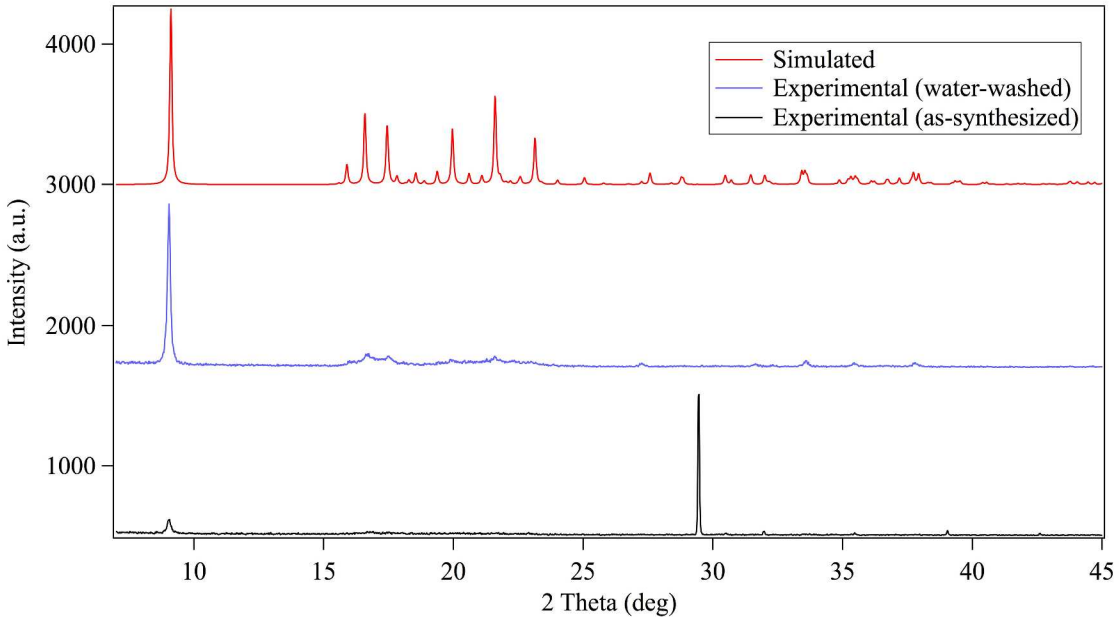


**Figure SI 29.** The simulated and experimental X-ray diffraction patterns of ZIF-7-III obtained from facile liquid-assisted mechanosynthesis.

## 10. Liquid-assisted mechanosynthesis, structure solution and Rietveld refinement of ZIF-9-III

*Synthesis*: Cobalt sulfate heptahydrate ($CoSO_4 \cdot 7H_2O$, 70.70 mg, 0.25 mmol), HPhIm (59.30 mg, 0.50 mmol) and $NaHCO_3$ (42.90 mg, 0.51 mmol) were mixed in an agate mortar. The reagents were then manually ground under ethanol for 10 minutes. After 2 days drying in air, the product was washed with water to get rid of remaining $NaHCO_3$ and $Na_2SO_4$. Violet powdery product was obtained for characterization. The XRPD pattern of ZIF-9-III is compared with the simulated pattern from the model given by Yang *et al*., 2008[12] after replacing Co in Zn site.

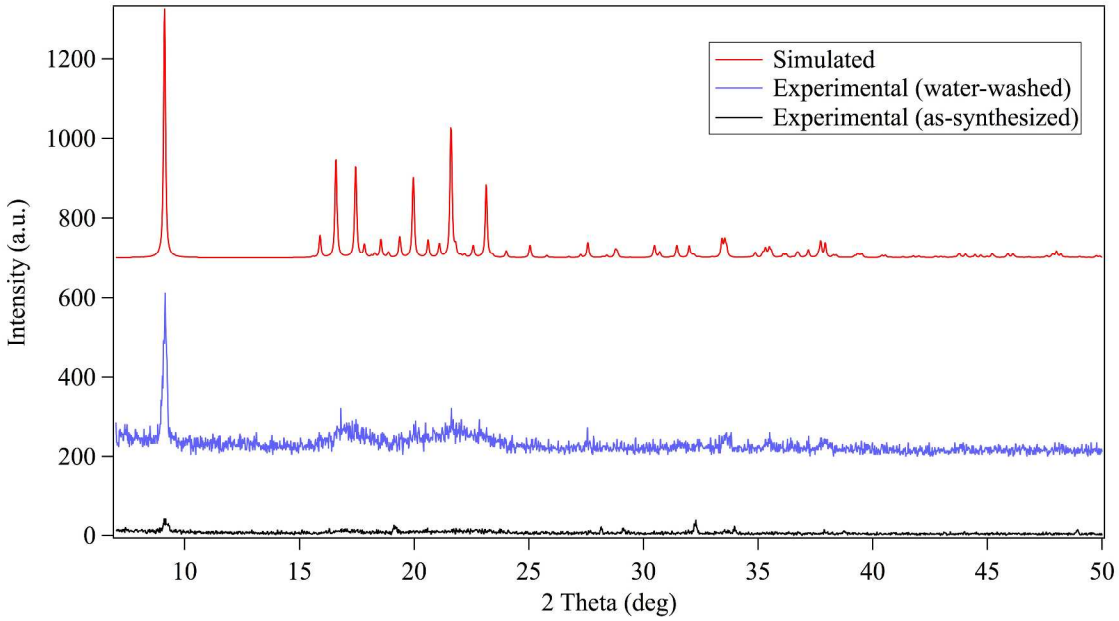


**Figure SI 30.** The simulated and experimental XRPD patterns of ZIF-9-III obtained from facile liquid-assisted mechanosynthesis.

*Data collection*: The ZIF-9-III crystal structure was confirmed by X-ray powder diffraction (XRPD) using Bruker D8 Advance X-ray diffractometer equipped with a Sol-X detector, parallel sollerslits, an incident beam monochromator with CuK$\alpha_1$ radiation ($\lambda$=1.5406 Å) and pulse height amplifier discrimination. The generator was operated at 40 kV and 40 mA. The sample was prepared for analysis by gently grinding the product obtained in an agate mortar and then depositing on a greased low background sample holder. Diffraction data were collected at room temperature in the range of 6-50° (2$\theta$), in $\theta$:2$\theta$ mode and step-scan with $\Delta$2$\theta$=0.03°, for 15 seconds per step.

*Structure solution and Rietveld refinement*: ZIF-7-III crystal structure was used as a starting model for the isomorphous ZIF-9-III structural refinement. The background and the peak shape were modeled with a 7-term shifted Chebyshev and a pseudo-Voigt function respectively. Spherical harmonics were used for preferred orientation correction. Benzimidazolate ligands

were treated as rigid bodies to reduce the number of variables. Single isotropic thermal factors were set for the ligands and cobalt element respectively.

**Table SI 3.** Crystal data and structure refinement of ZIF-9-III structure.

| | | |
|---|---|---|
| Empirical formula | $C_{14}H_{10}N_4Co$ | |
| Formula weight | 293.2 | |
| Temperature | 300 K | |
| Wavelength | 1.5406 Å | |
| Crystal system | Monoclinic | |
| Space group | *C*2/*c* | |
| Unit cell dimensions | *a*=16.106(1) Å<br>*b*=16.045(10) Å<br>*c*=19.51(1) Å | β= 96.62(6)° |
| Volume | 5008.7 $Å^3$ | |
| *Z* | 4 | |
| *Z*' | 4 | |
| Density | 1.555 $Mg/m^3$ | |
| 2θ range for data collection | 5-60° | |
| Index range (2θ) | 5-60° | |
| Refinement method | Rietveld refinement method | |
| $R_{wp}$ | 20.20% | |
| $R_{bragg}$ | 5.29% | |
| $Chi^2$ | 1.147 | |

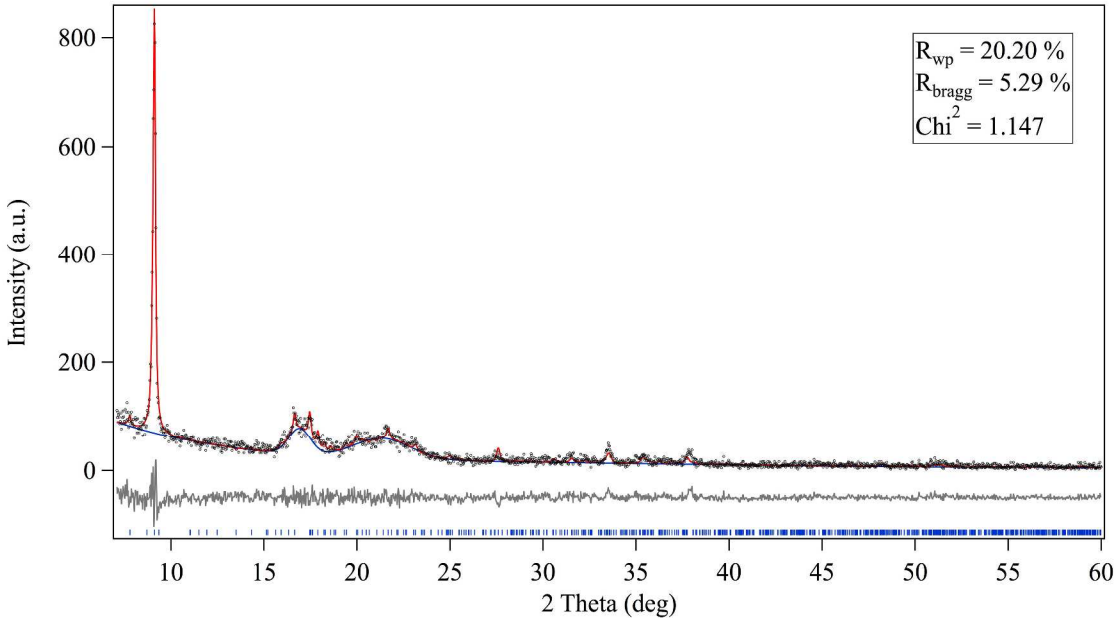


**Figure SI 31**. The observed and calculated XRPD patterns of ZIF-9-III.

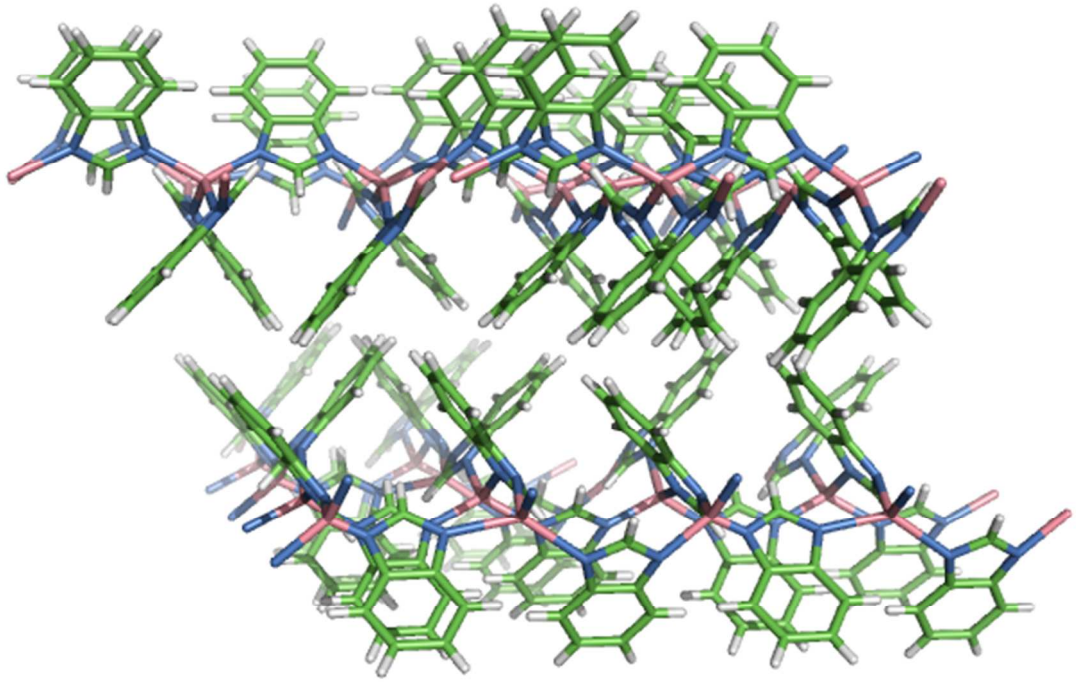

**Figure SI 32.** The structure of ZIF-9-III. Co: pink; N: blue; C: green; H: silver

**References:**


1. Gücüyener, C.; van den Bergh, J.; Gascon, J.; Kapteijn, F., *J. Am. Chem. Soc.* **2010**, 132 (50), 17704-17706.

2. Park, K. S.; Ni, Z.; Côté, A. P.; Choi, J. Y.; Huang, R.; Uribe-Romo, F. J.; Chae, H. K.; O'Keeffe, M.; Yaghi, O. M., *Proc. Natl. Acad. Sci. USA* **2006**, 103 (27), 10186-10191.

3. Coelho, A. A. TOPAS-Academic, 4.1; Coelho Software, Brisbane.: 2007.

4. Pawley, G., *J. Appl. Crystallogr.* **1981**, 14 (6), 357-361.

5. Miller, S. R.; Pearce, G. M.; Wright, P. A.; Bonino, F.; Chavan, S.; Bordiga, S.; Margiolaki, I.; Guillou, N.; Ferey, G.; Bourrelly, S.; Llewellyn, P. L., *J. Am. Chem. Soc.* **2008**, 130 (47), 15967-15981.

6. Material Studio, 4.3; Accelrys: San Diego, USA and Cambridge UK.

7. (a) McCusker, L. B.; Von Dreele, R. B.; Cox, D. E.; Louer, D.; Scardi, P., *J. Appl. Crystallogr.* **1999**, 32 (1), 36-50; (b) Young, R. A., Oxford University Press: 1995.

8. (a) Thompson, S. P.; Parker, J. E.; Potter, J.; Hill, T. P.; Birt, A.; Cobb, T. M.; Yuan, F.; Tang, C. C., *Rev. Sci. Inst.* **2009**, 80 (7), 75107-75109; (b) Parker, J. E., In *7th International Conference on Processing and Manufacturing of Advanced Materials , Materials Science Forum*, Vol. 706-709, pp 1707-1712.

9. Stephens, P., *J. Appl. Crystallogr.* **1999**, 32 (2), 281-289.

10. Blatov, V. A., *Struct. Chem.* **2012**, 23 (4), 955-963.

11. Xu, H. J.; Liu, Y. X.; Shen, Z.; Tian, Y. Q.; You, X. Z., Z. *Anorg. Allg. Chem.* **2005**, 631 (8), 1349-1351.

12. Yang, Q. F.; Cui, X. B.; Yu, J. H.; Lu, J.; Yu, X. Y.; Zhang, X.; Xu, J. Q.; Hou, Q.; Wang, T. G., *Cryst. Eng. Comm.* **2008**, 10 (11), 1534-1541.